Dynamics of Atmospheres and Oceans 45 (2008) 102–134

Contents lists available at ScienceDirect

Dynamics of Atmospheres and Oceans

journal homepage: www.elsevier.com/locate/dynatmoce

Steering of upper ocean currents and fronts by the topographically constrained abyssal circulation

Harley E. Hurlburt[a,*], E. Joseph Metzger[a], Patrick J. Hogan[a], Charles E. Tilburg[b], Jay F. Shriver[a]

[a] *Naval Research Laboratory, Stennis Space Center, MS 39529, USA*
[b] *University of New England, Biddeford, ME 04005, USA*

ARTICLE INFO

Article history:
Available online 6 July 2008

Keywords:
Ocean circulation
Western boundary currents
Oceanic fronts
Abyssal circulation
Bottom topography effects
Pacific Ocean
New Zealand region
Kuroshio region
Sea of Japan

ABSTRACT

A two-layer theory is used to investigate (1) the steering of upper ocean current pathways by topographically constrained abyssal currents that do not impinge on the bottom topography and (2) its application to upper ocean – topographic coupling via flow instabilities where topographically constrained eddy-driven deep mean flows in turn steer the mean pathways of upper ocean currents and associated fronts. In earlier studies the two-layer theory was applied to ocean models with low vertical resolution (2–6 layers). Here we investigate its relevance to complex ocean general circulation models (OGCMs) with high vertical resolution that are designed to simulate a wide range of ocean processes. The theory can be easily applied to models ranging from idealized to complex OGCMs, provided it is valid for the application. It can also be used in understanding some persistent features seen in observed ocean frontal pathways (over deep water) derived from satellite imagery and other data. To facilitate its application, a more thorough explanation of the theory is presented that emphasizes its range of validity. Three regions of the world ocean are used to investigate its application to eddy-resolving ocean models with high vertical resolution, including one where an assumption of the two-layer theory is violated. Results from the OGCMs with high vertical resolution are compared to those from models with low vertical resolution and to observations. In the Kuroshio region upper ocean – topographic coupling via flow instabilities and a modest seamount complex are used to explain the observed northward mean meander east of Japan

* Corresponding author. Tel.: +1 228 688 4626; fax: +1 228 688 4759.
E-mail addresses: hurlburt@nrlssc.navy.mil (H.E. Hurlburt), metzger@nrlssc.navy.mil (E.J. Metzger), hogan@nrlssc.navy.mil (P.J. Hogan), ctilburg@une.edu (C.E. Tilburg), shriver@nrlssc.navy.mil (J.F. Shriver).

0377-0265/$ – see front matter. Published by Elsevier B.V.
doi:10.1016/j.dynatmoce.2008.06.003

where the Kuroshio separates from the coast. The Japan/East Sea (JES) is used to demonstrate the impact of upper ocean – topographic coupling in a relatively weak flow regime. East of South Island, New Zealand, the Southland Current is an observed western boundary current that flows in a direction counter to the demands of Sverdrup flow and counter to the direction simulated in nonlinear global flat bottom and reduced gravity models. A model with high vertical resolution (and topography extending through any number of layers) and a model with low vertical resolution (and vertically compressed but otherwise realistic topography confined to the lowest layer) both simulate a Southland Current in the observed direction with dynamics depending on the configuration of the regional seafloor. However, the dynamics of these simulations are very different because the Campbell Plateau and Chatham Rise east and southeast of New Zealand are rare features of the world ocean where the topography intrudes into the stratified water column over a relatively broad area but lies deeper than the nominal 200 m depth of the continental shelf break, violating a limitation of the two-layer theory. Observations confirm the results from the high vertical resolution model. Overall, the model simulations show increasingly widespread upper ocean – topographic coupling via flow instabilities as the horizontal resolution of the ocean models is increased, but fine resolution of mesoscale variability and the associated flow instabilities are required to obtain sufficient coupling. As a result, this type of coupling is critical in distinguishing between eddy-resolving and eddy-permitting ocean models in regions where it occurs.

Published by Elsevier B.V.

1. Introduction

Different regions of the world ocean are used to investigate the roles that the topographically constrained abyssal circulation can play in steering the pathways of upper ocean currents (and associated fronts) when these currents do not directly impinge on the topography, especially the role of upper ocean – topographic coupling via flow instabilities. Key to the investigation is a two-layer theory that, unlike many theories, is easy to apply in analyzing the dynamics of ocean models ranging from highly idealized to complex eddy-resolving ocean general circulation models (OGCMs) with high vertical resolution that are designed for realistic simulation of a wide range of ocean processes. It is also useful in the interpretation of observations, especially persistent ocean frontal pathways (over the deep ocean) seen in satellite ocean imagery and ocean climatologies, as illustrated in this article, Hurlburt and Hogan (2008, this issue), and a number of the references cited below.

The two-layer theory has been used in studying the ocean dynamics of several regions, e.g. the Gulf of Mexico (Hurlburt and Thompson, 1980, 1982), the Gulf Stream (Hurlburt and Thompson, 1984; Thompson and Schmitz, 1989; Spall, 1996; Tansley and Marshall, 2000; Hurlburt and Hogan, 2008, this issue), the Kuroshio (Hurlburt et al., 1996; Hurlburt and Metzger, 1998), the Japan/East Sea (JES) (Hogan and Hurlburt, 2000, 2005), and the Australia–New Zealand region (Tilburg et al., 2001, 2002). Although the two-layer theory has been discussed to varying degrees in the preceding publications, here we present a more thorough explanation of the theory and its potential effects on current pathways, including its range of application and limitations, and specific situations where it does and does not apply. The studies cited above all used purely hydrodynamic ocean models with low vertical resolution (2–6 layers), some of them highly idealized, and all with the bottom topography confined to the lowest layer. In this article we investigate the applicability of the two-layer theory to complex OGCMs with high vertical resolution and realistic topography extending through any number of layers. We also compare results from such OGCMs with observations and with earlier results from models with low vertical resolution, specifically from studies cited above in the Kuroshio region, the

Japan/East Sea, and a region east of New Zealand, the last in a situation where the two-layer theory is violated.

Although abyssal currents driven by any mechanism can advect the pathways of upper ocean currents, upper ocean – topographic coupling via flow instabilities is an important example discussed in several of the references above, this article, and a companion paper (Hurlburt and Hogan, 2008, this issue). In this mechanism the pathways of eddy-driven abyssal currents are constrained by the geostrophic contours of the bottom topography and in turn steer the pathways of upper ocean currents. However, strong baroclinic instability is required to obtain sufficient coupling and increasingly widespread coupling is seen as the horizontal resolution is increased, based on collective evidence from Hurlburt et al. (1996), Hurlburt and Metzger (1998), Hogan and Hurlburt (2000), Tilburg et al. (2001), and Hurlburt and Hogan (2008, this issue), where the minimum resolution required ranges from 1/8° to 1/32° (14–3.5 km). Thus upper ocean – topographic coupling is a dynamical phenomenon that must be taken into account when distinguishing between eddy-permitting and eddy-resolving ocean models, the latter a subtopic discussed briefly in this article based on considering multiple dynamical phenomena and criteria.

In Section 2 we briefly discuss the ocean models with high and low vertical resolution used in this investigation. In Section 3 a two-layer theory for abyssal current steering of upper ocean current pathways is presented and its range of validity and limitations are discussed. In Section 4 three examples are used to test the hypothesis that a priori knowledge of the capabilities and limitations of the two-layer theory can be used to predict whether or not the theory will be consistent with simulations from an eddy-resolving ocean model with high vertical resolution. The summary, conclusions and some implications of the study are presented in Section 5, in particular implications of upper ocean – topographic coupling via flow instabilities (1) in distinguishing between eddy-permitting and eddy-resolving ocean models, and (2) its role in current separation from a western boundary in relation to other dynamics.

2. Ocean models used for the simulations

Two ocean models, the HYbrid Coordinate Ocean Model (HYCOM) and the Naval Research Laboratory (NRL) Layered Ocean Model (NLOM) were used for the simulations discussed herein. Both have a free surface and use a Lagrangian vertical coordinate to model the isopycnal ocean interior. Both allow isopycnal outcropping and strong diapycnal mixing, where that occurs, as well as weak diapycnal mixing in the ocean interior. However, the models differ dramatically in their complexity. Simplifications are made in NLOM which make it much more computationally efficient and often easier to understand, but which limit its range of application and versatility, while the generalized vertical coordinate and the allowance of zero thickness layers make HYCOM extremely versatile and suitable for almost any ocean modeling application where a hydrostatic model with a curvilinear, quadrilateral, quasi-horizontal grid is appropriate. In HYCOM, model-data comparisons are often easier than in NLOM, but analyzing and understanding the dynamics can be more challenging. Thus, it is valuable to have an approach to investigate abyssal current steering of upper ocean current pathways that is easily applied and understood.

General details of NLOM design and progressive development are discussed in Hurlburt and Thompson (1980), Wallcraft (1991), Wallcraft and Moore (1997), Moore and Wallcraft (1998), and Wallcraft et al. (2003). The last of these discusses the development of NLOM as a thermodynamic model with a mixed layer and sea surface temperature (SST). Although almost all of the NLOM simulations discussed here are hydrodynamic, the thermodynamic version of NLOM became the model component of the world's first eddy-resolving (1/16°) global ocean prediction system (Smedstad et al., 2003). It began running daily in real-time on 18 October 2000 and was run as an operational model by the Naval Oceanographic Office, Stennis Space Center, MS 27 September 2001 to 11 March 2006. On 6 March 2006, it was replaced by a 1/32° global NLOM prediction system discussed by Shriver et al. (2007). Real-time results from the 1/32° system and archived results from both systems can be seen on the web at http://www.ocean.nrlssc.navy.mil/global_nlom. A HYCOM-based eddy-resolving global ocean prediction system is a planned replacement for the existing system. A near real-time 1/12° Atlantic HYCOM prediction system has been running weekly since 2002 (Chassignet et al., 2006, 2007) and a

pre-operational 1/12° global HYCOM system has been running daily since 22 December 2006, both with results on the web at http://www.hycom.org (Hurlburt et al., 2008).

For NLOM simulations on a spherical grid (used in all but Section 3), the latitudinal and longitudinal resolution are constant when measured in degrees. The resolution is $1/x^\circ$ in latitude by $45/32x^\circ$ in longitude for each variable, e.g. $1/8^\circ \times 45/256^\circ$. For short, it is described by the latitudinal resolution. In NLOM the bottom topography is generally confined to the lowest layer and thus typically does not reach shallow depths except when NLOM is used as a single layer, barotropic model. Most of the simulations discussed here used vertically compressed but otherwise realistic bottom topography defined by

$$d_c = d_r + a_t(d - d_r), \tag{1}$$

where d_c is the depth of the compressed topography in the model, d_r is a reference depth, a_t is the fractional amplitude of the topography above d_r, and d is the depth without compression. Here $d_r = 6500$ m for the global and Pacific models and $d_r = 3750$ m for the Japan/East Sea, $a_t = 0$ for a flat bottom, $a_t = 1$ for uncompressed topography, and for simulations with variable-depth topography $a_t = .65$ in the global simulations, .80 in the Pacific simulation, and .85 or .90 in the JES simulations. Most shallow water regions are excluded except for some shallow straits. Sill depths of shallow straits are maintained by constraining flow to small values below the sill depth, e.g. see Metzger and Hurlburt (1996) for discussion. In regions where the two-layer theory is valid the reduced amplitude of the topography generally does not have significant impact on the abyssal current steering of upper ocean currents because even low amplitude topographic features constrain the pathways of abyssal flow (e.g. Hurlburt and Metzger, 1998), as in quasi-geostrophic models.

HYCOM was developed from the Miami Isopycnic Coordinate Ocean Model (MICOM) using the theoretical foundation set forth in Bleck and Boudra (1981), Bleck and Benjamin (1993), and Bleck (2002). HYCOM uses a generalized vertical coordinate that is normally isopycnal in the open stratified ocean, but which makes a dynamically smooth transition to pressure coordinates (nearly z-level) in the mixed layer and other unstratified or weakly stratified water, and to σ (terrain-following) coordinates in shallow water, although it is not limited to these coordinate choices. The transition between coordinate types is made dynamically in space and time using the layered continuity equation and a hybrid coordinate generator. The latter remaps Lagrangian perturbations in layer thickness toward a predetermined thickness when the layer density is different from a target density or when the layer thickness is less than a user-defined minimum, typically 1 m but nearly zero where layer interfaces intersect the bottom. This generalized coordinate approach retains particular advantages associated with the different vertical coordinate types: (1) the retention of water mass characteristics for centuries (a characteristic of the isopycnal coordinate interior), (2) high vertical resolution in the surface mixed layer and unstratified or weakly stratified regions of the ocean (a characteristic of z-level coordinates), and (3) high vertical resolution in coastal regions (a characteristic of terrain-following coordinates) (Chassignet et al., 2003). Another key feature of HYCOM is that it can have zero thickness layers, allowing isopycnals to intersect sloping topography, as in MICOM (Bleck and Smith, 1990). Where HYCOM uses pressure coordinates, partial cell topography is an automatic consequence of the generalized vertical coordinate design. Significant consequences of the HYCOM generalized coordinate approach are an unusual capability for accurate transition between deep and shallow water and the capability to use a sophisticated embedded mixed-layer model in an ocean model with an isopycnal interior. For HYCOM, the model resolution is x° by $x\cos(\text{latitude})^\circ$ for each variable and is described by the equatorial resolution regardless of the region modeled. Also, for "1/12°" HYCOM domains, the exact resolution is .08°. For comparison, 1/12° resolution in HYCOM $\simeq$ 1/16° resolution in NLOM at mid-latitudes, or ~7 km mid-latitude resolution for each variable.

3. Abyssal current steering of an upper ocean current pathway: theory and an illustrative application to a Loop Current simulation

We begin with an illustrative example of topographically constrained abyssal current steering of upper ocean currents obtained from idealized two-layer model results of Hurlburt and Thompson

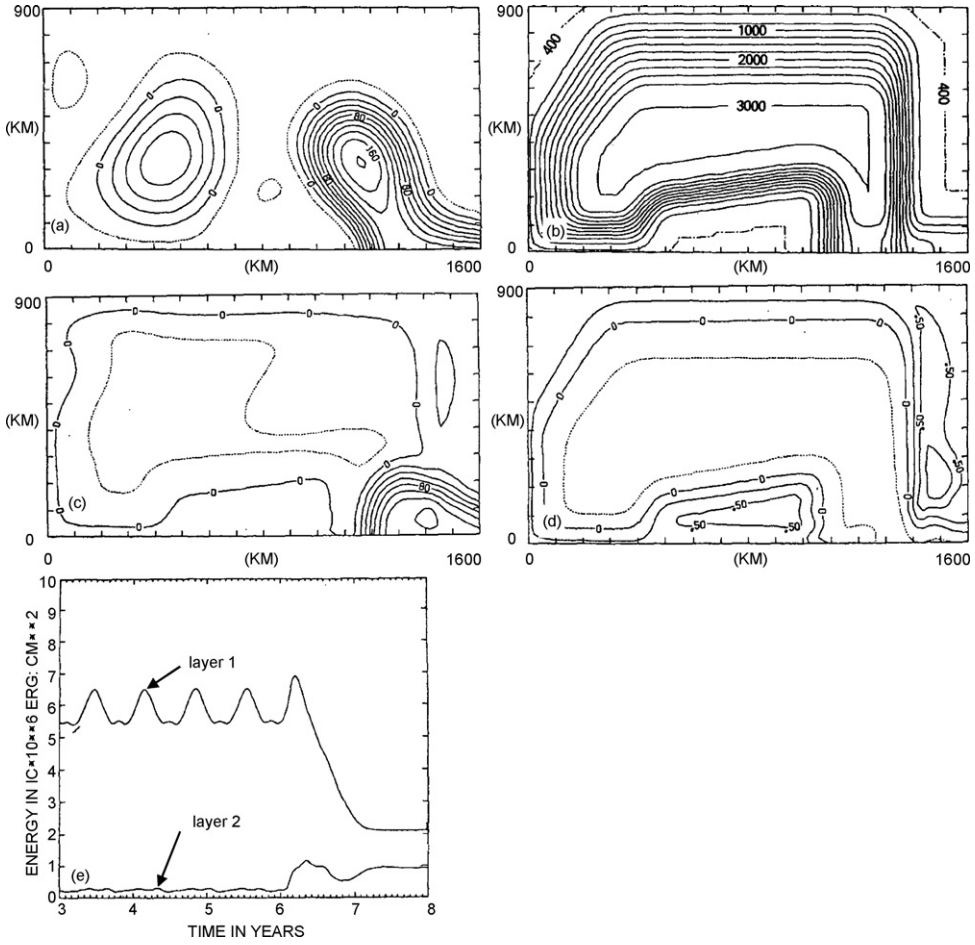

Fig. 1. Results from a two-layer idealized Gulf of Mexico model (a) snapshot of upper layer thickness anomaly at year 5.5 showing deep Loop Current penetration into the Gulf and an eddy previously shed by the Loop Current (contour interval = 20 m), (b) topographic depths varying from 400 to 3000 m with a contour interval of 250 m, (c) snapshot of the nearly steady upper layer thickness anomaly showing shallow Loop Current penetration into the Gulf and no eddies at year 8.0 (contour interval = 20 m), (d) snapshot of nearly steady lower layer pressure anomaly normalized by density at year 8.0 (contour interval = .25 $m^2\ s^{-2}$), and (e) domain-averaged kinetic energy vs. time for each layer (IC = 1.5). The inflow transport through the southern boundary is 25 Sv (1 Sv = $10^6\ m^3\ s^{-1}$) in the upper layer and zero in the lower layer until year 6, when it is increased to 10 Sv. The outflow transport matches the inflow transport in each layer. The mean upper layer thickness is 200 m. Adapted from Hurlburt and Thompson (1980).

(1980) (Fig. 1). The model included idealized bottom topography of the Gulf of Mexico confined to the lower layer (Fig. 1b). During the first 6 years of model integration the inflow through the southern port (25 Sv) was confined to the upper layer (layer 1) and regular eddy shedding from the model Loop Current occurred as illustrated in Fig. 1a and evidenced by the regular periodicity of the layer 1 kinetic energy (KE) curve (Fig. 1e). At the end of year 6 inflow through the southern port in the lower layer (layer 2) was added and gradually increased to 10 Sv with an e-folding time scale of 30 days. In response to this change, layer 2 KE increases but layer 1 KE decreases and both evolve to the steady state illustrated in Fig. 1c (upper layer thickness anomaly) and Fig. 1d (lower layer density normalized pressure anomaly). Fig. 1d shows that the lower layer inflow follows the geostrophic contours of the bottom topography anticyclonically around the basin. Along the eastern continental slope the abyssal

current is southward and intersects the remnant of the Loop Current at nearly a right angle before both exit through the eastern boundary.

Clearly, the southward abyssal current is preventing the northward penetration of the Loop Current illustrated in Fig. 1a. A number of approaches can be used to explain this result. Hurlburt and Thompson (1980) used a mass transport vorticity balance approach like that of Holland (1973), but they also used a particularly clear and direct approach based on the layered continuity equation and geostrophy in a two-layer model, one that showed how lower layer currents could advect the *pathways* of upper layer currents in the model.

In a two-layer model with no diapycnal mixing, the continuity equation for layer 1 is

$$h_{1t} + \boldsymbol{v}_1 \cdot \nabla h_1 + h_1 \nabla \cdot \boldsymbol{v}_1 = 0 \tag{2}$$

where h_1 is upper layer thickness, t is the time derivative and $\mathbf{v}_i$ is the velocity in layer i. The geostrophic component of the advective term in (2) can be related to the geostrophic velocity in layer 2 by

$$\boldsymbol{v}_{1g} \cdot \nabla h_1 = \boldsymbol{v}_{2g} \cdot \nabla h_1 \tag{3}$$

because from geostrophy,

$$\boldsymbol{k} \times f(\boldsymbol{v}_{1g} - \boldsymbol{v}_{2g}) = -g' \nabla h_1, \tag{4}$$

$\mathbf{v}_{1g} - \mathbf{v}_{2g}$ is parallel to contours of h_1. In (4) $\mathbf{k}$ is a unit vector, $f = 2\omega \sin\theta$ is the Coriolis parameter, ω is the Earth's rotation rate ($7.292 \times 10^{-5}\,\mathrm{s}^{-1}$), θ is latitude, $g' = g(\rho_2 - \rho_1)/\rho_2$ is the reduced gravity due to buoyancy, $g = 9.8\,\mathrm{m\,s}^{-2}$ is the gravitational acceleration of the Earth, and ρ_i is the water density in layer i. Since geostrophy is typically a very good approximation outside the equatorial wave guide and normally near surface flows are much stronger than abyssal ocean flows, then usually $|\mathbf{v}_1| \rangle\rangle |\mathbf{v}_2|$, making ∇h_1 a good measure of $\mathbf{v}_1$ under these conditions.

A significant conclusion from the preceding discussion is that geostrophically balanced abyssal currents advect upper layer thickness gradients and therefore can advect the pathways of upper layer currents in a two-layer model, especially where relatively strong abyssal currents intersect upper layer currents at large angles, as in the two-layer Gulf of Mexico example of Hurlburt and Thompson (1980). In their case the Loop Current had already penetrated far into the Gulf before layer 2 inflow through the Yucatan Channel was increased. When this increase occurred, the strength of the advection in Eq. (3) associated with the southward current along the continental slope in layer 2 began to exceed the magnitude of the divergence term in the continuity equation (Eq. (2)) where the Loop Current crossed the shelf slope, causing the interface between the two layers to shallow there. Thus, the Loop Current began to retreat southward until a balance between advection and divergence occurred in the continuity equation (Eq. (2)) near the southern end of the shelf, as illustrated in Fig. 28 of Hurlburt and Thompson (1980). Why this local southward advection prevented northward penetration of the entire Loop Current is explained dynamically in Hurlburt and Thompson (1980, 1982).

While the abyssal current steering had a powerful impact in this two-layer example, one might wonder if this strong abyssal current steering of upper ocean current pathways is an artifact of a two-layer model and question its applicability to an ocean model with higher vertical resolution. Clearly, the two-layer theory (1) is designed to explain abyssal current steering of upper ocean current pathways when the upper currents do not directly impinge on the bottom topography, and (2) does not apply when the topography significantly intrudes into the stratified ocean, in which case the flow would be directly steered by the geostrophic contours of the topography, as illustrated in Section 4.3. However, because of the bi-modal depth distribution in the world ocean, 7.6% shallower than 200 m, 85.9% deeper than 1500 m (in the 2′ DBDB2 topography; Ko, 2002), typically with steeply sloping topography in between, topographic intrusion into the stratified ocean is not an issue in most areas of the deep ocean, as illustrated in Fig. 2. As additional limitations, the theory (3) does not apply when higher vertical modes are important (Hurlburt et al., 1996) and (4) does not apply when ageostrophic flow has substantial impact. Thus, this two-layer theory is not likely to be useful in the tropics, where higher vertical modes and ageostrophic flows are more significant. Diapycnal mixing, time dependence, and in means of time-dependent flow, the length of the mean and eddy-mean components of the advection may also affect the results.

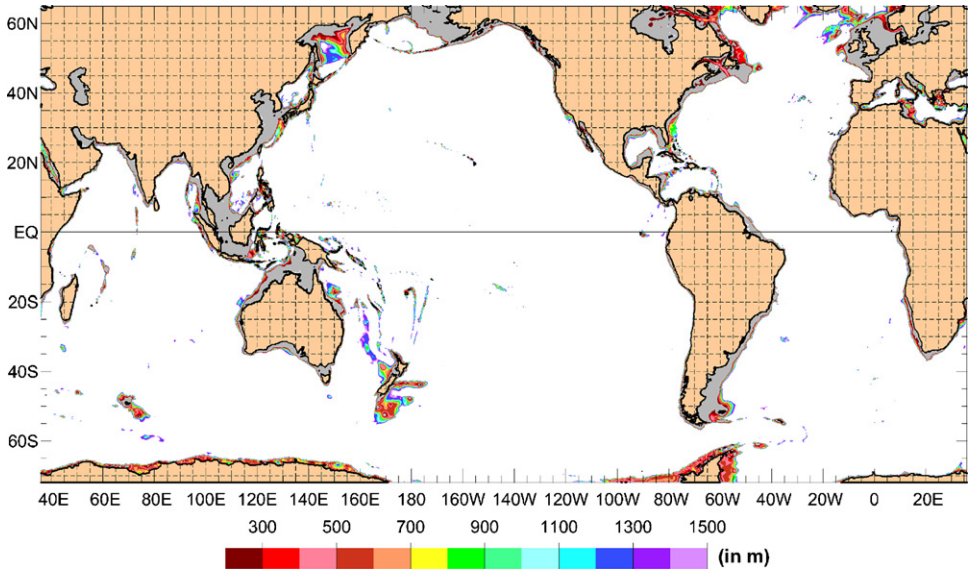

Fig. 2. Global map of topographic depths between 200 m and 1500 m, which comprise only 6.5% of the seafloor. The Campbell Plateau and Chatham Rise adjacent to New Zealand and the northern Sea of Okhotsk are relatively large regions with depths in this range. Depths <200 m are gray and >1500 m are white.

In the remainder of this study, the versatility and range of application of the theory are discussed using results from ocean model simulations with more than two layers, especially its application to upper ocean – topographic coupling via flow instabilities (Hurlburt et al., 1996) and boundary current separation from the coast. Baroclinic instability is particularly important because of its capability to drive deep mean flows by transferring energy from above the pycnocline into the abyssal ocean (Holland and Lin, 1975). In the Loop Current example just discussed, the abyssal and upper ocean current remained at large angles throughout the current pathway advection process, which was ultimately halted when a balance occurred between advection and divergence in the continuity Eq. (2). However, in examples discussed later, often a consequence of the abyssal current steering is abyssal and upper ocean currents that become more nearly parallel, since the current pathway advection is reduced when this occurs. This process results in a tendency towards barotropy.

4. Application of the two-layer theory to abyssal current steering of upper ocean current pathways in ocean models with high vertical resolution and to upper ocean – topographic coupling via flow instabilities

Simulating the mean pathways of ocean currents has proven to be an exceptionally challenging problem for ocean modelers in many cases, especially their pathways near separation from the coast and their extensions into the ocean interior. In many cases abyssal current steering of upper ocean currents plays an important role, but with many variations in the way it affects the circulation dynamics. Details of the coastline geometry and the bottom topography are often critical to the simulated pathway, in addition to the wind forcing and a number of dynamical mechanisms. These details limit the use of idealized models in gaining a clear understanding, as demonstrated for the Gulf Stream by Hurlburt and Hogan (2008, this issue).

Abyssal currents that steer upper ocean current pathways are typically driven either by vertical mixing or by flow instabilities. The former can be remotely driven, e.g. the global meridional overturning circulation as an extreme example. The eddy-driven abyssal currents derive from baroclinic instability (typically a mixed barotropic–baroclinic instability), which is very efficient in transferring

energy into the abyssal ocean (Holland and Lin, 1975; Holland, 1978). When abyssal currents driven by flow instabilities steer upper ocean current pathways, the process is termed upper ocean – topographic coupling via flow instabilities. This process requires that flow instabilities be well-resolved and thus an eddy-resolving not just an eddy-permitting ocean model. As a result, it is very useful in distinguishing between eddy-resolving and eddy-permitting ocean model simulations. Eddy-driven abyssal currents can extend well beyond regions of strong flow instabilities, as indicated by results in the subtropical Atlantic from Hurlburt and Hogan (2000) (their Figs. 9–13). They can even be important in steering upper ocean current pathways in weak flow regimes, such as the Japan/East Sea (Hogan and Hurlburt, 2000, 2005).

Earlier studies have applied the two-layer theory in Section 3 to abyssal current steering of upper ocean current pathways, but typically these studies have used ocean models with two to six layers in the vertical and topography confined to the abyssal layer, as in NLOM. In this section we investigate application of the two-layer theory to a model with high vertical resolution, HYCOM, which allows the bottom topography to extend through any number of layers. In particular, we test the hypothesis that a priori knowledge of the capabilities and limitations of the two-layer theory presented in Section 3 can be used to predict whether or not the theory will be consistent with eddy-resolving simulations from ocean models with high vertical resolution. Simulations of three regions are used to test this hypothesis, two where a priori knowledge indicates that the simulations should be consistent with the theory and thus the theory should be useful in explaining their dynamics (the Kuroshio just east of Japan and the Japan/East Sea), and a third example where topography intrudes well into the stratified water column over a substantial area, a clear violation of the theory (the Southland Current east of South Island, New Zealand).

In each example the hypothesis is tested (1) by comparing new results from high vertical resolution eddy-resolving HYCOM simulations with previously published results from low vertical resolution eddy-resolving NLOM simulations, and (2) by discussing how the two-layer theory did or did not apply in explaining the related ocean dynamics in each case. In the example where the theory is violated, a new dynamical explanation of the Southland Current and the pathway of the South Subtropical Front east of New Zealand is presented based on a HYCOM simulation and comparisons to recently published observational evidence. The reader is referred to the original publications for in-depth discussion of previously published results, as only the most pertinent results are discussed here. However, the new explanation for the Southland Current system is discussed in more detail.

4.1. The dynamics of upper ocean – topographic coupling via flow instabilities with application to the Kuroshio near Japan

The Kuroshio is a region with strong flow instabilities, an inertial jet that extends far into the basin, and strong interactions with the subarctic front. In addition, the subarctic front and a front associated with the Kuroshio Extension span most of the North Pacific. Realistic simulation and understanding of these features has been a challenge for ocean modelers, including features such as the straight path and the different meandering pathways south of Japan, the mean meanders immediately to the east of Japan, and the bifurcation of the Kuroshio Extension at the Shatsky Rise with the northern branch connecting to the subarctic front, as some more specific examples.

Here, we focus on the mean meanders east of Japan, the dynamics associated with their formation, and the sensitivity of simulations to the horizontal and vertical resolution and to the bottom topography. A 20-layer HYCOM simulation and three six-layer NLOM simulations are used for this purpose, all covering the Pacific Ocean and its marginal seas north of 20°S. The HYCOM simulation used monthly climatological forcing based on the European Centre for Medium-Range Weather Forecasts (ECMWF) Reanalysis over 1979–1993 (ERA15) (Gibson et al., 1997). The wind stress and the latent and sensible heat fluxes were calculated using the 10 m winds and other variables via the bulk formulation of Kara et al. (2002). Most of the NLOM simulations were forced by the monthly Hellerman and Rosenstein (1983) (HR) wind stress climatology after it was smoothed once with a nine-point filter on the original 2° grid (designated HRsm) to eliminate severe noise with a 4° wavelength that was found in the wind stress curl when the unsmoothed winds were interpolated to the model grid.

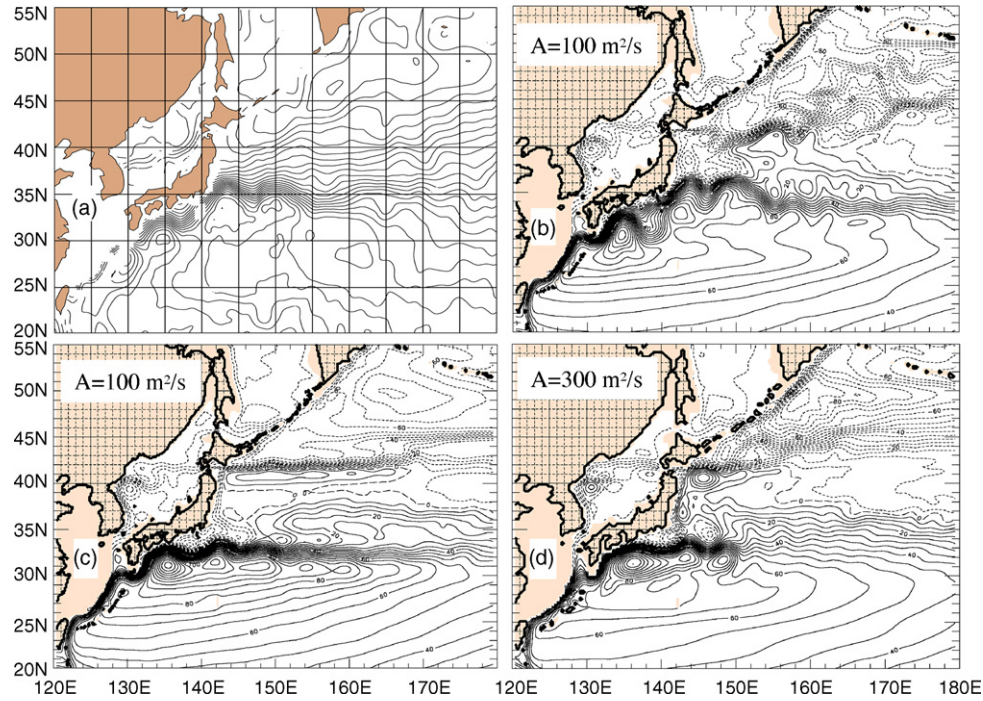

Fig. 3. (a) Mean surface dynamic height relative to 1000 m from version 2.5 of the Generalized Digital Environmental Model (GDEM) oceanic climatology, an update of the version described by Teague et al. (1990). (b–d) Mean SSH in the Northwest Pacific from three Pacific NLOM simulations north of 20°S. (b) 1/8°, six-layer nonlinear with realistic bottom topography, (c) 1/8°, six-layer nonlinear flat bottom, and (d) 1/4°, six-layer nonlinear with realistic topography. All were forced by the HRsm wind stress climatology. A is the horizontal eddy viscosity. The contour interval is 5 cm in all panels. (b) and (c) are from Hurlburt et al. (1996) and (d) from Hurlburt et al. (1997).

Fig. 3 depicts the mean SSH in the northwestern Pacific from three NLOM simulations in comparison to the mean surface dynamic height with respect to 1000 m from the Generalized Digital Environmental Model (GDEM) oceanic climatology (an update of the version described by Teague et al., 1990). The 1/4° (Fig. 3d) and 1/8° (Fig. 3b) simulations with bottom topography are identical in design except for the horizontal grid resolution and the eddy viscosity coefficient (A). The two 1/8° simulations are identical except that one has a flat bottom (Fig. 3c) and the other (Fig. 3b) has vertically compressed but otherwise realistic bottom topography confined to the lowest layer. In all of the simulations, flow is constrained to small values below the sill depth in straits, e.g. the shallow straits connecting the Japan/East Sea to the Pacific basin. This constraint was also applied to the flat bottom simulation to avoid having unrealistic currents through marginal seas influence the simulation of the Pacific Ocean. Comparing the eddy-permitting 1/4° simulation with bottom topography (Fig. 3d) and the 1/8° flat bottom simulation (Fig. 3c) and focusing on the Kuroshio pathway south and east of Japan to about 150°E, where the simulations are strongly inertial, one might arrive at the false conclusion that the bottom topography is not important. In this region their simulated Kuroshio pathways agree closely, including the latitude of the mean current pathway and the amplitudes and longitudes of the meander crests and troughs. Further, the latitude of the simulated jets (centered along 33.5°N) is consistent with the demands of Sverdrup flow from the HRsm wind stress climatology (shown in Hurlburt et al., 1996). In contrast, comparison of the two 1/8° simulations demonstrates a large topographic impact with a 3° northward displacement in the Kuroshio pathway east of Japan, giving much better agreement with the pathway in the GDEM climatology.

Dynamics of the topographic impact on the Kuroshio separation from the coast and its pathway east of Japan are illustrated in Fig. 4 using the same 1/8° simulation with bottom topography and a

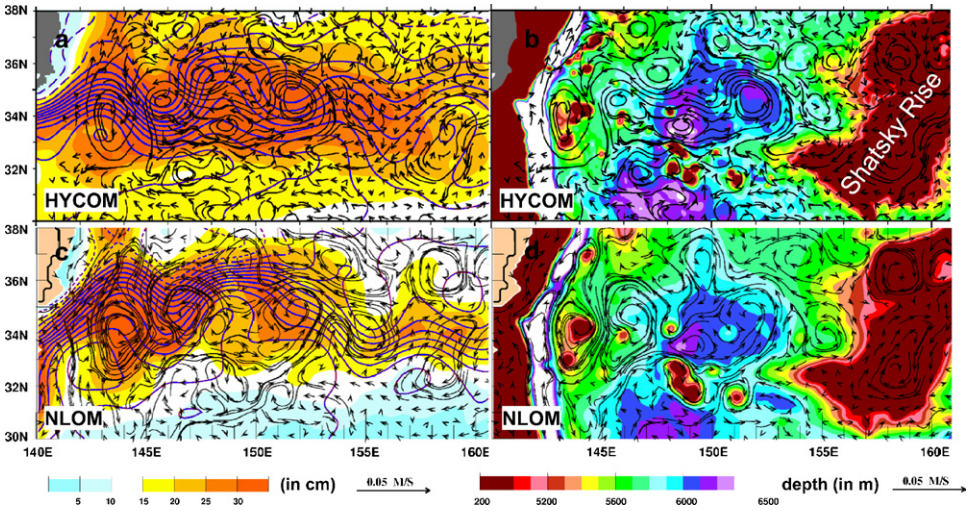

Fig. 4. Results from the Kuroshio Extension region east of Japan. Results from (a and b) 20-layer, 1/12° Pacific HYCOM north of 20°S and (c and d) the same 1/8°, six-layer Pacific NLOM simulation with realistic bottom topography shown in Fig. 3b; (a and c) mean SSH (blue contours with a 7.5 cm contour interval) and mean abyssal currents (arrows) overlaid on rms SSH variability, and (b and d) mean abyssal currents overlaid on the bottom topography. Blank areas in the abyssal currents exist where the HYCOM topography extends above layer 19, the layer used to depict them. In HYCOM density increments between deep layers are very small and the Kuroshio lies above the topographic features. Panels c and d were adapted from Hurlburt et al. (1996). Digital output from the NLOM simulation is no longer available to permit a quantitative comparison with the HYCOM results.

1/12° Pacific HYCOM simulation. Fig. 4a (HYCOM) and Fig. 4c (NLOM) depict the Kuroshio (red contours of mean sea surface height) and abyssal currents (black arrows) overlaid on a background of rms SSH variability that indicates regions of high variability, mainly due to flow instabilities, in shades of orange. Fig. 4b (HYCOM) and Fig. 4d (NLOM) depict the abyssal currents overlaid on the bottom topography. In essence, the Kuroshio Extension exhibits a mixed barotropic–baroclinic instability that transfers energy from the upper ocean to the abyssal layer. The abyssal flow is constrained by the geostrophic contours of the bottom topography (Fig. 4b and d). In turn, the abyssal currents can steer upper ocean currents as discussed in Section 3. The preceding process is an example of upper ocean – topographic coupling via flow instabilities (Hurlburt et al., 1996). Even fairly small, low amplitude topographic features demonstrate a substantial effect in steering the pathway of the simulated Kuroshio Extension east of Japan. In particular, a modest seamount chain east of the trench (in white) along 143–144°E appears to play a major role in creating the observed mean northward meander just east of Japan and in the northward shift of the Kuroshio pathway east of Japan, influencing the Kuroshio separation from the coast. The model mean abyssal currents in this area are corroborated by deep current meter measurements from the Kuroshio Extension Regional Experiment (WOCE line PCM7) (Hallock and Teague, 1996), including a southward deep western boundary current along the west side of the trench (where in HYCOM the topography is shallower than the layer depicted).

In the 1/4° simulation the flow instabilities, abyssal currents, and abyssal eddy kinetic energy (EKE) are much weaker and hence the upper ocean – topographic coupling via the flow instabilities is weaker and insufficient to produce a realistic Kuroshio pathway. However, once the horizontal resolution is sufficient to support flow instabilities strong enough to give upper ocean – topographic coupling, as in Fig. 4, the results show low sensitivity to the horizontal resolution (~7 km in 1/12° HYCOM, ~14 km in 1/8° NLOM) or the vertical resolution. Consistent with the 2-layer theory, 20-layer HYCOM and 6-layer NLOM yield essentially the same results for upper ocean – topographic coupling via flow instabilities east of Japan, including the eddy-driven mean abyssal currents and the steering of the mean Kuroshio meanders, indicating flow dominated by barotropic and lowest vertical mode baroclinic dynamics in both models. In addition, there is low sensitivity to the treatment of bottom topography, full amplitude extending through any number of layers in HYCOM vs. vertically compressed and confined to the lowest

layer in NLOM. There is also low sensitivity to the choice of atmospheric forcing in this case and low sensitivity of the fields depicted to the presence or absence of thermodynamics and thermal forcing, present in HYCOM while the NLOM simulation is purely hydrodynamic (thermodynamics and thermal forcing are included in some NLOM simulations, e.g. Wallcraft et al. (2003) and in the NLOM-based eddy-resolving global ocean prediction systems (Smedstad et al., 2003; Shriver et al., 2007)).

While Hurlburt et al. (1996) found that 1/8° (∼14 km) resolution was sufficient to model the observed mean meanders just east of Japan, Hurlburt and Metzger (1998) found that 1/16° resolution and a strong inertial jet penetrating far enough to the east were needed to simulate the bifurcation of the Kuroshio at the Shatsky Rise, which they explained using upper ocean – topographic coupling via flow instabilities. In this region higher resolution was required to obtain an eddy-resolving simulation that (1) simulated sufficient eastward inertial jet penetration and (2) flow instabilities strong enough to obtain upper ocean – topographic coupling. Since the first internal Rossby radius of deformation, commonly used to distinguish between eddy-resolving and eddy-permitting ocean models, does not vary much along the Kuroshio Extension east of Japan (Emery et al., 1984; Chelton et al., 1998), the ability to realistically simulate inertial jets is a second criterion for distinguishing between eddy-permitting and eddy-resolving ocean models. In both locations along the Kuroshio Extension east of Japan, upper ocean – topographic coupling via flow instabilities was a key measure in distinguishing between eddy-permitting and eddy-resolving simulations.

4.2. The Japan/East Sea: upper ocean – topographic coupling in a weak flow regime

Compared to the western boundary currents of the subtropical gyres in major ocean basins, the currents in the Japan/East Sea are relatively weak with typical transports of 1–3 Sv (Preller and Hogan, 1998; Chang et al., 2004) and the internal Rossby radius of deformation is relatively small (Oh et al., 2000). Thus, the JES provides an example of upper ocean – topographic coupling via flow instabilities and the associated abyssal current steering of upper ocean current pathways in a much weaker flow regime. Hogan and Hurlburt (2000, 2005) also investigated the impact of wind forcing choice on the simulated dynamics. The preceding studies used four-layer hydrodynamic simulations by NLOM with inflow through the Tsushima Strait and outflow through the Tsugaru and Soya Straits (labeled in Fig. 5a). Two layers are open through Tsushima and Tsugaru, but only the top layer through Soya, consistent with the sill depths. Hogan and Hurlburt (2006) used a 15-layer HYCOM simulation to investigate the formation of intrathermocline eddies (ITEs) in the JES, features not simulated by NLOM.

Here, we use model-data comparisons and results from both HYCOM and NLOM to investigate (1) the relevance of the two-layer theory for abyssal current steering of upper ocean current pathways and (2) the role of upper ocean – topographic coupling via flow instabilities in a model with high vertical resolution in the presence of a weak flow regime. As part of this effort we investigate (a) whether the HYCOM simulation agrees best with the NLOM simulation using the same wind forcing and (b) whether the upper ocean circulation of the NLOM simulation using the same wind forcing as HYCOM agrees better with HYCOM than with the NLOM simulations using different wind forcing.

Hogan and Hurlburt (2000) performed a resolution convergence study using NLOM at 1/8° (∼14 km), 1/16°, 1/32° and 1/64° resolution. They found the increase from 1/16° to 1/32° resolution had a profound basin-wide impact on the simulated circulation in both the upper ocean and in the abyssal ocean, but the further increase to 1/64° resolution had a much smaller impact, demonstrating close to resolution convergence at 1/32° in the simulated surface and abyssal circulations over most of the JES. In Fig. 6 the surface (a) and abyssal currents (b) from a four-layer 1/32° NLOM simulation forced by the HRsm monthly wind stress climatology are overlain on the bottom topography, clearly demonstrating the basin-wide impact of upper ocean – topographic coupling via flow instabilities on the surface circulation, a result not seen at lower resolution. The tendency toward barotropy as a result of the topographic steering is clearly evident with the mean surface circulation paralleling the abyssal circulation and the topographic slopes in many locations, e.g. the pathway of the mean subpolar front in the model, which spans the JES from western boundary current separation to the Tsugaru Strait outflow along 40 ± 1.5°N in this simulation and the schematic (Fig. 5a). Another example is the

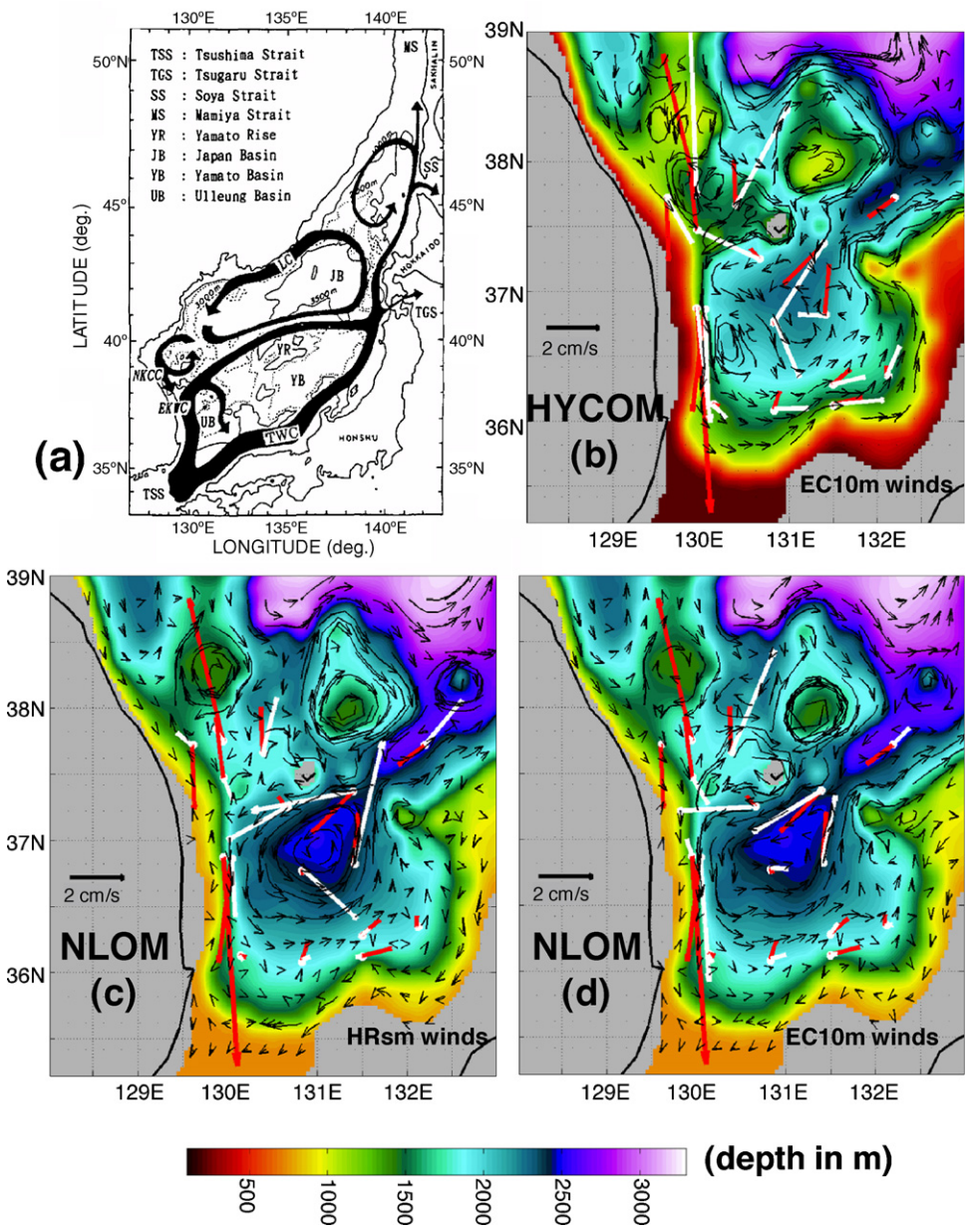

Fig. 5. (a) Schematic map of surface currents in the Japan/East Sea (JES) from Morimoto and Yanagi (2001), after Senyu (1999), reproduced with permission of the Oceanographic Society of Japan, copyright holder. (b–d) Observed mean abyssal currents from Chang et al. (2002, 2004) and Teague et al. (2005) in red and co-located model mean abyssal currents in white superimposed on additional JES model mean abyssal currents in black and the bottom topography in color. The simulations were forced by monthly mean wind stress climatologies, (b) 1/25° HYCOM with EC10M, (c) 1/32° NLOM with HRsm, and (d) 1/32° NLOM with EC10M. The corresponding vector correlations between the simulated and observed mean abyssal currents are (b) .76, (c) .28 and (d) .33. All three simulations have ~3.5 km resolution in the JES.

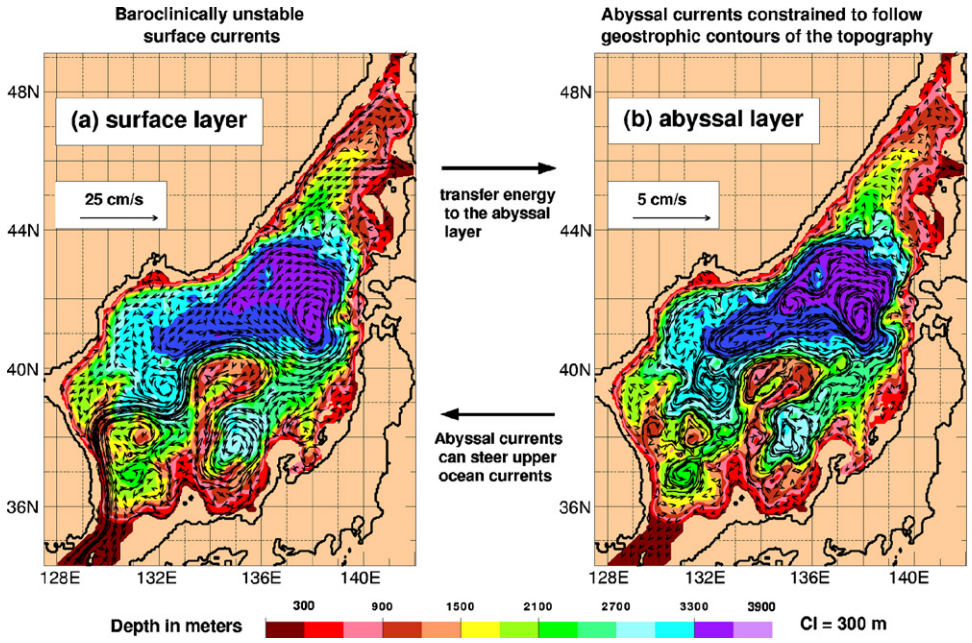

Fig. 6. Results from a 1/32° Japan/East Sea (JES) NLOM simulation forced by HRsm. Bottom topography and mean currents for (a) the surface layer and (b) the abyssal layer. This figure illustrates the dynamics of upper ocean – topographic coupling via mesoscale flow instabilities (mixed baroclinic–barotropic). From Hogan and Hurlburt (2000).

mean eddy (Ulleung Eddy) centered over a topographic rise just south of the subpolar front near 38°N, 131.3°E and close to the location of a persistent eddy observed by Gordon et al. (2002) which was an ITE during an observing period in May 1999, but which had lost its intrathermocline characteristics the following January, a phenomenon simulated by HYCOM (Hogan and Hurlburt, 2006).

As evident in Fig. 6 the modeled East Korea Warm Current (EKWC) (labeled in Fig. 5a) sharply separates from the coast of Korea and connects with the subpolar front above a rise in the topography centered at 38.4°N, 129.5°E. Hogan and Hurlburt (2000) found that the rise is crucial to EKWC separation in this simulation. When the rise is removed, the EKWC continues farther north along the coast and separates from the coast too far north, as in the lower resolution simulations. They also found EKWC separation too far north in otherwise identical 1/32° flat bottom and reduced gravity simulations, the latter having an infinitely deep, inert abyssal layer.

While the 1/32° model forced by the HRsm monthly wind stress climatology and prescribed flow through the straits simulated the surface circulation in good agreement with the schematic based on observational data (Fig. 5a), Hogan and Hurlburt (2005) found the choice of wind stress forcing product could have a substantial impact on the mean circulation and its dynamics as simulated by the 1/32° model, even with the strong topographic constraints (Fig. 7). Despite the differences, 5 of the 6 wind products give JES simulations in generally good agreement with the schematic, but the National Centers for Environmental Prediction (NCEP) reanalysis (Kalnay et al., 1996) is an outlier by driving a very unrealistic simulation with the EKWC extending extremely far northward. In the HRsm and European Centre for Medium-Range Weather Forecasts (ECMWF) 1000 mb (EC1000) (Gibson et al., 1997) forced simulations, EKWC separation from the coast depends on upper ocean – topographic coupling and a specific topographic rise, but the ECMWF 10 m (EC10M), Na (Na et al., 1992, 1999) and Fleet Numerical Meteorology and Oceanography Center (FNMOC) (Rosmond et al., 2002) forced simulations give an EKWC separation pathway that passes southeast of the rise and does not depend on the rise topography. In those simulations EKWC separation from the coast depends primarily on

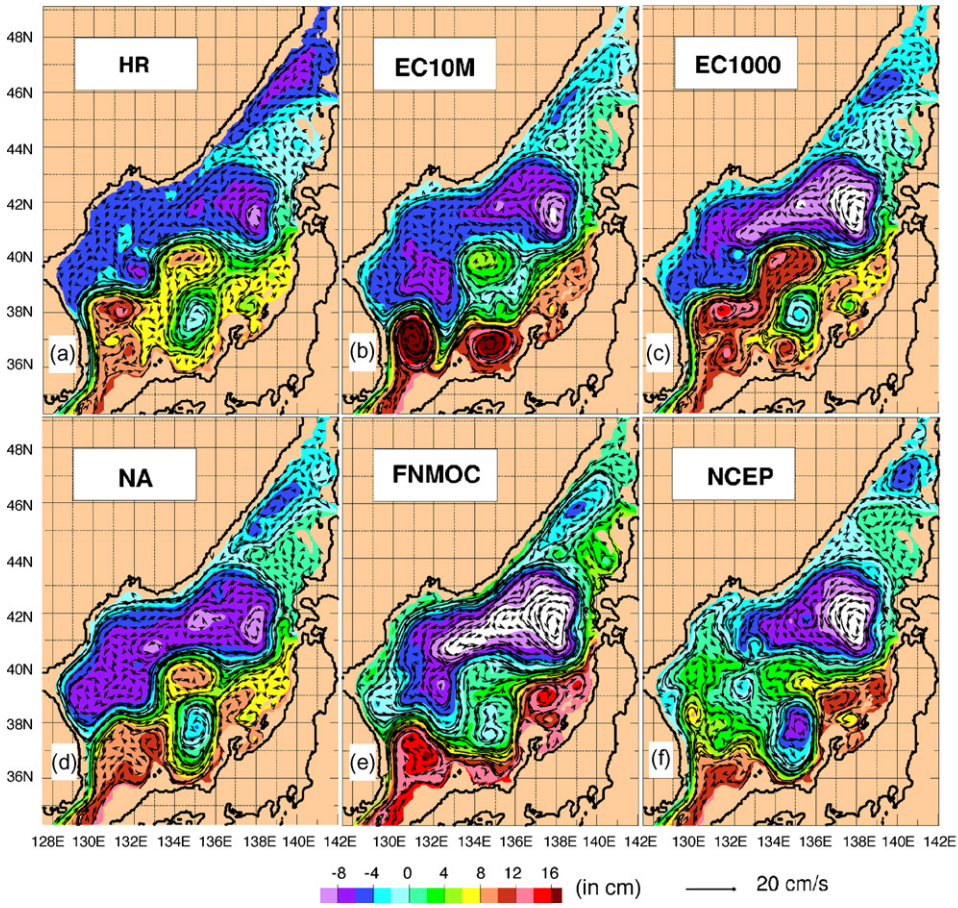

Fig. 7. Mean SSH (color) and currents (vectors) from four-layer 1/32° nonlinear JES NLOM simulations forced by prescribed seasonally varying flow in through the Tsushima Strait (mean 2 Sv) and out through the Tsugaru Strait (2/3) and the Soya Strait (1/3) and by wind stress forcing from (a) HRsm, (b) EC10M, (c) EC1000, (d) Na, (e) FNMOC and (f) NCEP. Contour interval for SSH is 1 cm. See Hogan and Hurlburt (2005) for discussion of the atmospheric forcing products over the Japan/East Sea and the text for explanation of the nomenclature. All are monthly wind stress climatologies. From Hogan and Hurlburt (2005).

the distribution of positive wind stress curl (Hogan and Hurlburt, 2005, their Fig. 2) and the existence of the Tsushima Warm Current (TWC, labeled in Fig. 5a), seen off the northern coast of Japan in all of the simulations, as explained in detail by Hogan and Hurlburt (2005). These three wind forcing products, especially Na, have relatively large areas of positive wind stress curl in the northern JES, allowing simulations where EKWC separation from the coast does not depend on upper ocean – topographic coupling. However, in all of the simulations upper ocean – topographic coupling strongly influences the pathway of the subpolar front after EKWC separation and many other features of the circulation.

Hogan and Hurlburt (2005) also presented results from corresponding eddy-permitting 1/8° simulations. Except for the FNMOC-forced simulation, all of the 1/32° simulations show marked differences from their 1/8° counterparts. The FNMOC-forced simulation had much greater isopycnal outcropping and vertical mixing extending to the abyssal layer. In the other simulations, the abyssal circulation was very weak at 1/8° resolution, but in the 1/8° FNMOC-forced simulation vertical mixing drove an abyssal circulation strong enough to steer the upper ocean current pathways.

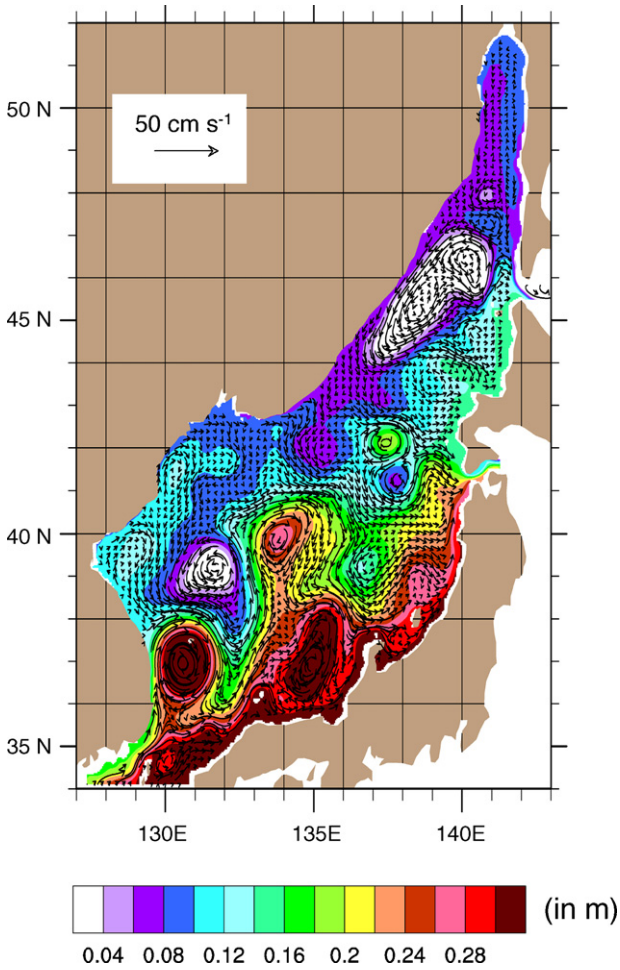

Fig. 8. Mean SSH (color) and currents (vectors) from a 15-layer 1/25° HYCOM Japan/East Sea simulation forced by the same EC10M monthly wind stress climatology used for the four-layer simulation in Fig. 7b and the same mean inflow and outflow transports. Both the 4- and 15-layer simulations have ~3.5 km horizontal resolution. Modified from Hogan and Hurlburt (2006).

The mean surface layer circulation from the six 1/32° 4-layer NLOM simulations (Fig. 7) are compared to that from a 15-layer, 1/25° HYCOM simulation with nearly the same horizontal resolution (~3.5 km) (Fig. 8), the latter a simulation used by Hogan and Hurlburt (2006) to investigate the dynamics of ITE formation. HYCOM allows the topography to extend through any number of the layers. The simulation results from the two models agree quite closely when both use the same wind forcing (EC10M) (Fig. 7b vs. Fig. 8), more closely than the four-layer simulations driven by the other five wind products (Fig. 7). That includes the mean pathway of the subpolar front, its mean meanders and the adjacent mean eddies/gyres.

Table 1 contains a quantitative comparison between the HYCOM simulation with EC10M wind forcing (Fig. 8) and the six NLOM simulations with different wind forcing (Fig. 7). Only the region south of 41°N, the nominal northern edge of the subpolar front, is used in these comparisons. That region is more baroclinic and contains the stronger baroclinic currents. The latitudinal restriction also avoids inflation of the SSH correlations because the SSH north of 41°N tends to be relatively low overall compared to south of 41°N. The SSH correlation and the vector correlation for near surface currents

Table 1
Dependence of model–model comparisons on the choice of atmospheric forcing product in the Japan/East Sea south of 41°N

	HYCOM/EC10M vs. NLOM			NLOM/EC10M vs. NLOM/other		
	SSH correlation	Near surface current vector correlation HYCOM L2 vs. NLOM L1	Deep current vector correlation HYCOM L14 vs. NLOM L4	SSH correlation	Near surface current vector correlation for NLOM L1	Deep current vector correlation for NLOM L4
NLOM/HRsm	.58	.32	.69	.62	.39	.84
NLOM/EC10M	.83	.61	.72	–	–	–
NLOM/EC1000	.58	.33	.75	.60	.47	.89
NLOM/NA	.67	.29	.76	.70	.44	.92
NLOM/FNMOC	.67	.40	.76	.83	.61	.90
NLOM/NCEP	.24	.13	.75	.42	.21	.86

The model and atmospheric forcing product are indicated by model/wind forcing. Counting from the surface down, HYCOM has 15 layers and NLOM has 4 and the layer number is indicated by L*x*. To calculate the correlations in this table, the HYCOM values were interpolated to the NLOM grid.

are highest for the HYCOM and NLOM simulations with the same atmospheric forcing, corroborating the result from visual inspection. Further, these simulations agree better than the NLOM simulation with EC10M forcing agrees with the NLOM simulations forced by other wind products, except for equal agreement with the FNMOC-forced simulation. The NLOM simulation with NCEP forcing is the outlier both visually and quantitatively. Due to the topographic constraint (Fig. 5b–d) the deep vector correlations in Table 1 are generally higher than the near surface correlations and show low sensitivity to the choice of atmospheric forcing product. With a vector correlation of .76 the mean bottom layer (layer 15) currents simulated by HYCOM are in good agreement with measured mean abyssal currents reported by Chang et al. (2002, 2004) and Teague et al. (2005) (Fig. 5b). The corresponding correlations with the mean abyssal (layer 4) currents simulated by NLOM are lower, .33 with the EC10M wind forcing and .28 with HRsm forcing, but the mean abyssal layer currents simulated by NLOM agree quite well with mean currents one layer higher in HYCOM (layer 14, Table 1), yielding a vector correlation of .72 south of 41°N when both use the EC10M wind forcing.

With limited variability in location, the mean anticyclonic eddies south of the subpolar front became ITEs in HYCOM during much of the year, when the mixed layer was shallow (Hogan and Hurlburt, 2006). The pathway of the subpolar front around the mean eddy associated with EKWC separation agrees closely with the position of the Ulleung Eddy as described by Chang et al. (2004) and is almost 1° south of the Ulleung Eddy and ITE observed by Gordon et al. (2002) in May, 1999 and January, 2000. Like the four-layer NLOM EC10M simulation, HYCOM simulates a relatively strong Tsushima Warm Current and relatively weak currents along the subpolar front. The model inter-comparison results and the model-data comparisons indicate that the two-layer theory for abyssal current steering of upper ocean current pathways and the related upper ocean – topographic coupling via flow instabilities made a large contribution to the relevance of the four-layer hydrodynamic model in helping to understand the dynamics of the Japan/East Sea and simulations by a more complex model with higher vertical resolution, even though the four-layer model could not simulate the ITE aspect of eddies that was studied by Hogan and Hurlburt (2006) using HYCOM.

4.3. Remote topographic forcing of a baroclinic western boundary current, an explanation for the Southland Current and the pathway of the south subtropical front east of New Zealand?

Tilburg et al. (2002) present an explanation for the Southland Current, a northeastward western boundary current along the east coast of South Island, New Zealand, and the pathway of the south subtropical front east of New Zealand. The explanation is based on remote topographic forcing due to a deep western boundary current along the eastern edge of the Campbell Plateau, which occupies the southeast quadrant off South Island, NZ. The 1/8° global NLOM simulation used by Tilburg et al. has vertically compressed but otherwise realistic bottom topography confined to the lowest layer. However, parts of the Campbell Plateau extend into the stratified water column, violating a limitation of the two-layer theory (Section 3) used as part of the explanation. Here, we summarize the theory and results of Tilburg et al. (2002) and then use HYCOM to investigate how full amplitude topography modifies the results and test the applicability of the theory.

The Southland Current flows along a segment of the south subtropical front that turns eastward along the south side of the Chatham Rise and returns southward ~12° east of New Zealand, as indicated by the observed wide wedge of cold SST protruding northward east of South Island (Fig. 9a adapted from Uddstrom and Oien, 1999). Fig. 9b–d compare a schematic of the regional currents and fronts from Sutton (2001) (Fig. 9b) with mean near surface currents simulated by 1/12° global HYCOM with 32 layers, thermobaricity and a reference depth of 2 km for potential density (Fig. 9c) and a seven-layer, 1/32° global NLOM configuration (Fig. 9d) that is thermodynamic with a mixed layer and SST (Wallcraft et al., 2003; Kara et al., 2003; Kara and Hurlburt, 2006). See Chassignet et al. (2003) for a discussion of reference density and thermobaricity in HYCOM. The NLOM configuration is the model component of an operational data-assimilative eddy-resolving global ocean prediction system (Shriver et al., 2007), but here with climatological atmospheric forcing and no ocean data assimilation. The global HYCOM configuration is its planned replacement. The wind forcing for the 1/32° NLOM simulation is the HR monthly wind stress climatology and for HYCOM a monthly wind stress climatology based on (a)

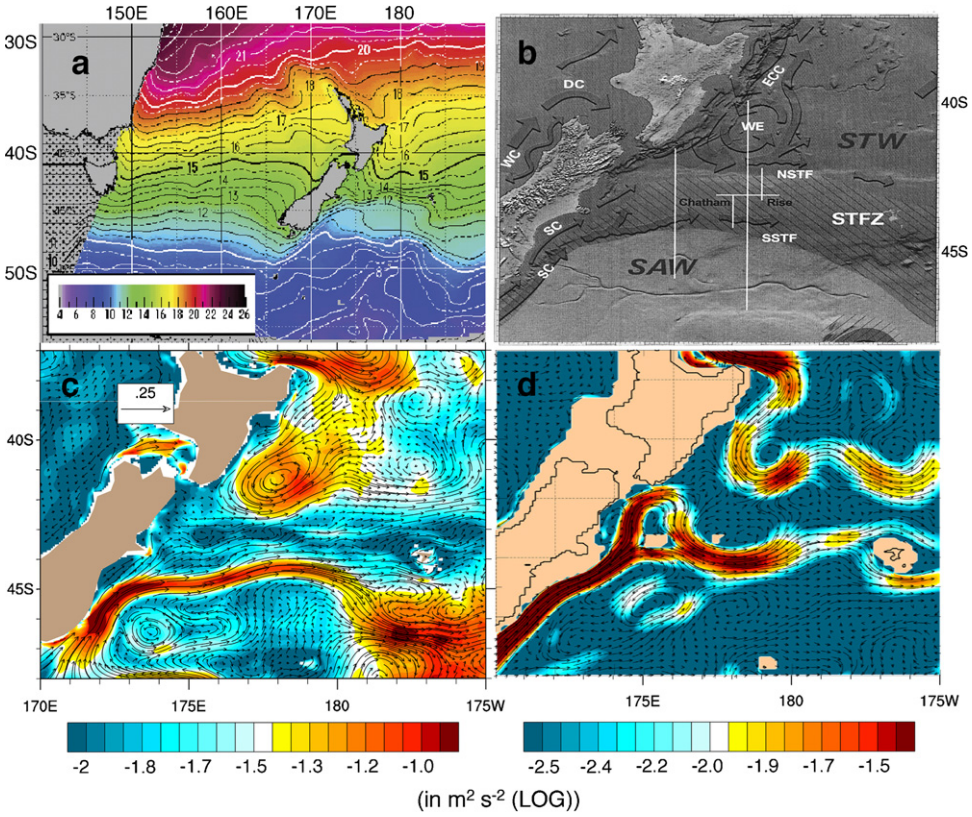

Fig. 9. (a) Annual mean SST (°C) surrounding New Zealand computed over 5 years, January 1993 to December 1997, compiled by Uddstrom and Oien (1999). The pathway of the Subantarctic Front (SAF) generally follows the 8–8.5 °C isotherms. The south subtropical front (SSTF) is more complex. It is associated with the 12–13 °C isotherms west of New Zealand and the 11–13 °C isotherms directly east of New Zealand, but its southward dip near 53°S, 173°W is evident in the 9–9.5 °C isotherms. (b) Schematic of mean currents and fronts east of New Zealand from Sutton (2001). The subtropical frontal zone (STFZ) separates subtropical water (STW) and subantarctic water (SAW). See text for additional nomenclature. (c) Mean layer three currents centered 8.6 m deep (arrows) overlaid on kinetic energy of the mean flow (KEM) (color) from a 1/12°, 32-layer global HYCOM simulation forced using an ECMWF ERA40 monthly climatology with wind speed modified using QuikSCAT (see text). (d) Mean surface layer currents (arrows) overlaid on KEM (color) from a 1/32° global NLOM simulation with thermodynamics and seven layers, including the mixed layer. The model was forced by the HR monthly wind stress climatology. (a) was modified and (b) reproduced with permission of the American Geophysical Union, copyright holder.

ECMWF ERA40 10 m winds (Kallberg et al., 2004) with the wind speed corrected using a monthly climatology from QuikSCAT scatterometer data and (b) the bulk formulation of Kara et al. (2005) for converting the 10 m winds to wind stress.

Both models demonstrate good agreement with Sutton's schematic, including part of the Southland Current (SC) turning eastward along the path of the south subtropical front (SSTF) on the south side of the Chatham Rise and part continuing northward through a channel at the west end of the Chatham Rise to the north end of South Island. North of the Chatham Rise they simulate the East Cape Current (ECC), Wairapa Eddy (WE) and an eastward current along the north subtropical front (NSTF) on the north side of the Chatham Rise (phenomena investigated by Tilburg et al., 2001). Thus, both models simulate the observed dual eastward currents and double front on each side of the Chatham Rise. The double subtropical frontal structure (NSTF and SSTF) in the South Pacific originates on the north and south sides of the Chatham Rise. It was discovered in data from Dmitry Mendeleev cruise 34 (Belkin, 1988) and is shown in the context of the global southern

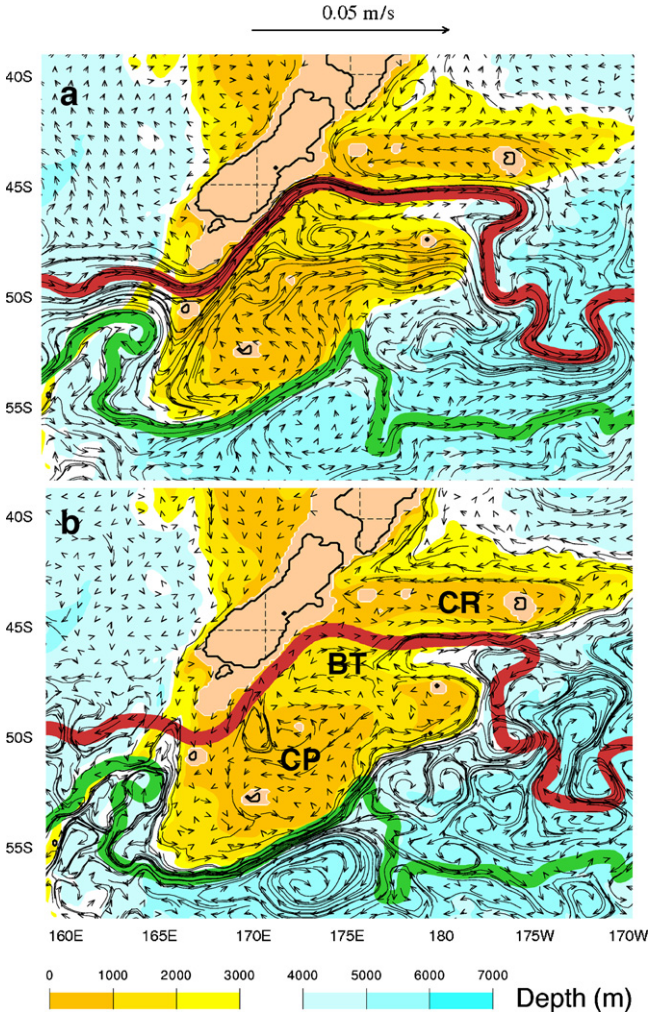

Fig. 10. (a) Mean surface layer currents overlaid on the bottom topography from a 1/8°, six-layer nonlinear global NLOM simulation and (b) mean abyssal currents from the same simulation overlaid on the topography. The simulated pathways of the SSTF (heavy red line) and the SAF (heavy green line) are also overlaid. From Tilburg et al. (2002). The model Chatham Rise (CR) and Campbell Plateau (CP) (in shades of orange) lie east and southeast of South Island, NZ, respectively. The Bounty Trough (BT) lies between them.

ocean frontal structure by Belkin and Gordon (1996). The simulated westward flow on the north side of the Chatham Rise is a deficiency in the 1/8° global NLOM simulation used by Tilburg et al. (2002) in studying the dynamics of the SC and the pathway of the SSTF (Fig. 10a), but one not material to the topic under investigation. The deficiency is not present in the corresponding 1/16° and 1/32° global NLOM simulations used by Tilburg et al. (2001) or in Fig. 9d. The higher resolution global NLOM configurations simulate the SC and SSTF in a manner similar to 1/8° global NLOM.

The Southland Current has an unusual dynamical property in that it is a western boundary current that flows opposite to the direction predicted by a linear model with a Sverdrup (1947) interior, Munk (1950) western boundary layers and that is consistent with the theory of Godfrey (1989) for including islands, here calculated using a global 1/16° linear numerical model forced by the modified ERA40

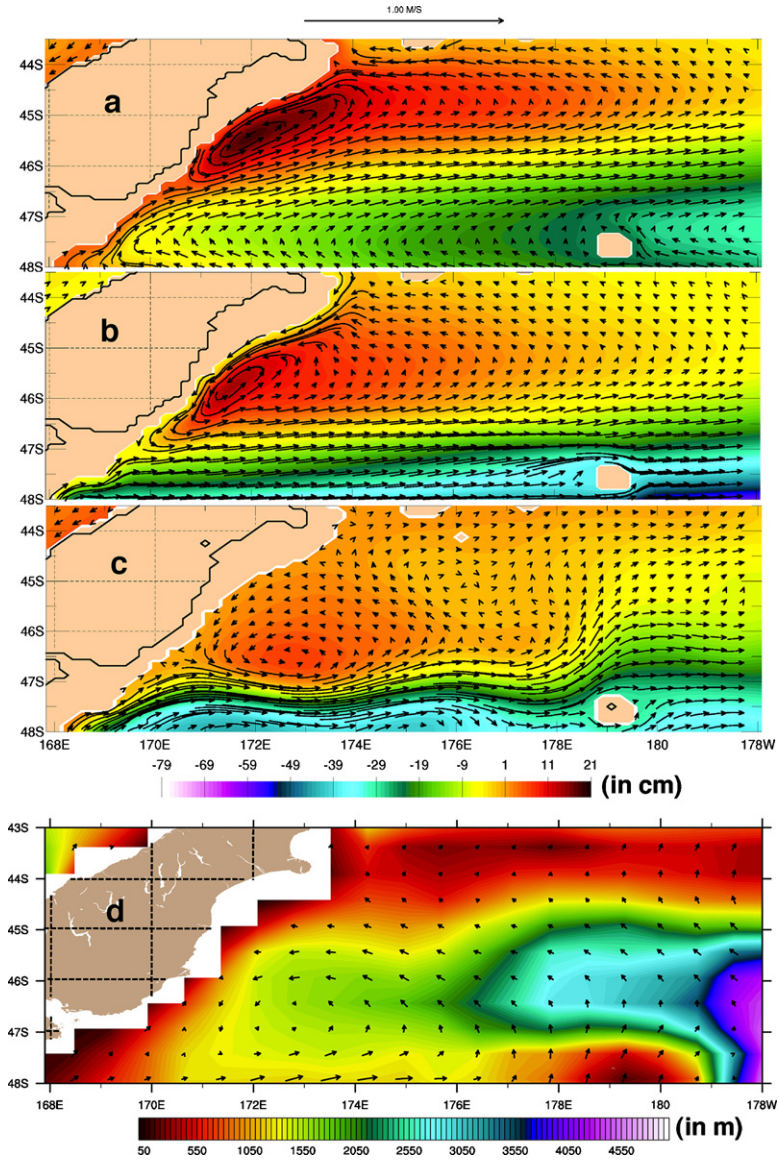

Fig. 11. Mean currents and SSH east of South Island, NZ from linear 1/16° global NLOM simulations: (a) with the modified ECMWF winds used to force 1/12° and .72° global HYCOM (see text) and (b) the HRsm wind stress climatology used in forcing 1/8° global NLOM. (c) Mean surface layer currents and SSH from a 1/8°, six-layer global nonlinear NLOM simulation with a flat bottom. A corresponding 5.5-layer nonlinear reduced gravity simulation shown in Tilburg et al. (2001; their Fig. 9b) also depicts a similar, but stronger, anticyclonic gyre in this region. (d) Mean currents at 8.6 m depth from .72° global HYCOM overlaid on the model bottom topography.

wind stress used in forcing global HYCOM (Fig. 11a) and by the HRsm wind stress (Fig. 11b) used in forcing the 1/8° global NLOM simulations. In accord with the linear theory, a nonlinear 1/8° global flat bottom NLOM simulation forced by HRsm also reverses the Southland Current to southwestward (Fig. 11c) as does a .72° version of the global HYCOM simulation (56 km resolution at 45.5°S) with the modified ERA40 wind forcing and realistic seafloor topography (Fig. 11d). When vertically compressed

but otherwise realistic bottom topography is added to the nonlinear 1/8° global NLOM (the same two 1/8° nonlinear simulations used by Tilburg et al., 2001), the simulation switches to the observed northeastward direction of the Southland Current (Fig. 10a).

Fig. 10b reveals no local abyssal current steering that might explain how adding realistic topography would cause a current that flows counter to linear theory. What are the dynamics responsible for the existence of the Southland Current and the northward excursion of the SSTF? Tilburg et al. (2002) offer remote topographic forcing of a baroclinic western boundary current as an explanation. Although there is no local abyssal current steering, the model simulates an abyssal current along the southeastern edge of the Campbell Plateau consistent with observational/modeling studies of a South Pacific Deep Western Boundary Current (DWBC) by Moore and Wilkin (1998) and Carter and Wilkin (1999). Despite weak flow instabilities, the 1/8° global NLOM simulates a robust DWBC because of diapycnal mixing and subduction along outcropping isopycnals that extend deeply into the ocean interior. Tilburg et al. (2002) find that this DWBC, which crosses the SSTF 12° east of New Zealand, is crucial to the existence of the Southland Current. Their explanation of the Southland Current, as due to remote topographic forcing, is a new dynamical mechanism for generation of a baroclinic western boundary current. Specifically, the DWBC locally advects the SSTF northward to the southern edge of the Chatham Rise where the perturbation propagates westward as a nondispersive first internal Rossby wave until it reaches the east coast of South Island, NZ. There it equilibrates forming a baroclinic western boundary current to satisfy the northward advection of the SSTF ∼12° to the east.

The process of forming a baroclinic western boundary current via remote topographic forcing is illustrated in Fig. 12 using an idealized two-layer model with 1/2° resolution. Fig. 12a shows the model configuration with eastward inflow (5 Sv) through a port in the western boundary and outflow at the same latitude in the eastern boundary. With no flow through boundaries in the lower layer, the model was run to the zonal jet equilibrium state shown in the upper layer streamfunction of Fig. 12b. Starting from the equilibrium state of Fig. 12b, meridional northward flow (20 Sv based on observations of the South Pacific DWBC below 2000 m; Moore and Wilkin, 1998) was introduced through the ports in the lower layer. This flow was dynamically constrained to follow the geostrophic contours of the topography with an idealized Campbell Plateau to the west. The abyssal current locally advected the pathway of the upper ocean current northward (Fig. 12c) and the perturbation propagated westward (Fig. 12d) to form a baroclinic western boundary current in the equilibrated state (Fig. 12e), consistent with the explanation of the results in Fig. 10. As the upper ocean current passed over the northward abyssal flow, it returned to its previous latitude, creating a pathway corresponding to that observed by Uddstrom and Oien (1999).

Fig. 13 depicts mean currents from 1/12° global HYCOM with 32 layers in the vertical. The ECMWF atmospheric forcing is from ECMWF-ERA40 (Kallberg et al., 2004) with the modified wind stress described earlier. Mean currents from three layers, layer 3 (a fixed depth layer centered at 8.6 m), layer 15 (a nearly isopycnal layer centered near 400 m depth) and layer 27 (an isopycnal layer centered near 3300 m depth) are overlaid on the HYCOM bottom topography. HYCOM simulates a Southland Current/SSTF pathway, a subantarctic front (SAF) pathway and a South Pacific DWBC pathway that have similarities to those found in NLOM by Tilburg et al. (2002) (Fig. 10). However, there are significant differences. Most notably, HYCOM simulates two pathways feeding the Southland Current, (1) a shallow pathway approaching South Island, NZ from the southwest (Fig. 13a) that is similar to the pathway in NLOM (Fig. 10a) and (2) a deeper pathway approaching from the east along ∼48°S (Fig. 13a and b) not simulated by NLOM.

To help illustrate the origin of the deeper pathway, Fig. 14 depicts the vertical structure of currents normal to five cross-sections from HYCOM marked in Fig. 13a. The deeper pathway in HYCOM is fed from the boundary current along the southeastern edge of the Campbell Plateau, a current that extends to the bottom at depths down to nearly 5000 m, but which also has a strong baroclinic component (Fig. 14a). A portion of this current along isobaths <∼1200 m deep separates from the portion located above deeper isobaths and proceeds through a passage in the Campbell Plateau with a sill depth of ∼1200 m (Fig. 14c), while the remainder continues east-northeastward along the Campbell Plateau minus most of the flow above isobaths shallower than 1200 m (Fig. 14b). The shallower branch then flows westward to South Island, NZ along a slope in the Campbell Plateau between the ∼800 m and ∼1300 m isobaths (centered near the 1100 m isobath) (Fig. 14e). From Fig. 14e this flow has a

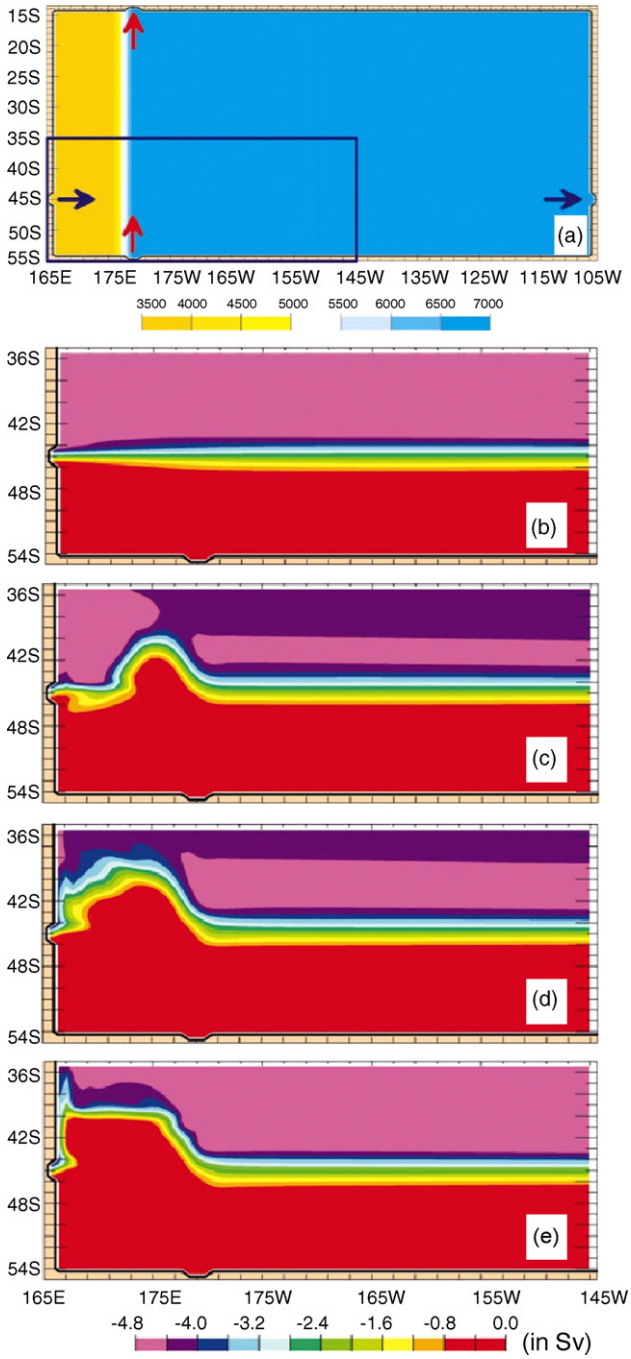

Fig. 12. Idealized simulation of the SSTF pathway and Southland Current formation east of New Zealand via remote topographic forcing. (a) Domain and bottom topography (color in meters) of the two-layer model. The red arrows represent flow through ports in the lower layer, simulating the South Pacific Deep Western Boundary Current. The blue arrows represent flow through ports in the upper layer, simulating flow associated with the SSTF. The shallow topography in the western portion of the model domain represents an idealized Campbell Plateau. The blue rectangle outlines the region displayed in the remaining figure panels.

substantial barotropic component. The current continues along the geostrophic contours of the Bounty Trough, which lies between the Campbell Plateau and the Chatham Rise, turning northeastward as a major component of the Southland Current along South Island, NZ (Fig. 14d), then eastward along the southern edge of the Chatham Rise and the SSTF until a portion separates from the Rise and returns southward just west of the dateline. The remainder of the eastward current separates from the Chatham Rise in a U-turn near 176.5°W. The first separation (Fig. 13a and b) occurs where there is convex curvature in the Chatham Rise (Fig. 13c). The remainder of the current separates where isobaths converge and sharp steepening of the Chatham Rise slope occurs south of Chatham Island (44°S, 176.5°W). The isobath convergence and slope steepening are best seen in Fig. 13c and they cause a narrowing of the north-south width of the depth range beneath the eastward current at the separation longitude (Fig. 13a and b).

When the westward current, along the southern edge of the Bounty Trough (∼48°S), nears South Island, NZ, it feeds into the Southland Current and merges with its shallow component inshore of the SSTF, the latter indicated by flow above shallow topography in Fig. 14d and in the eastward flow along ∼45°S (Fig. 14e). Along the southern edge of the Chatham Rise, the current also becomes more baroclinic and is centered over slightly deeper isobaths (∼1300 m) (Fig. 14e) vs. ∼1100 m in Fig. 14b–d. Based on a mean from eight hydrographic sections, Sutton (2003) found a mean steric transport of 8.3 Sv for the Southland Current, using the bottom as a level of no motion. The 1/12° global HYCOM simulation gives a mean steric transport of 9.0 Sv at 46.5°S (Fig. 14d) in close agreement with Sutton's mean, but in the 1/12° HYCOM simulation ∼60% of the Southland Current transport is non-steric (13.2 Sv) for a total of 22.2 Sv.

The westward current along ∼48°S feeding into the Southland Current and the eastward flow along the SSTF on the south side of the Chatham Rise are clearly supported by the observationally based SSH mean of Maximenko and Niiler (2005) (see also Niiler et al., 2003), as seen in a regional zoom (Fig. 15a) in comparison to simulated mean SSH in the region from 1/12° global HYCOM (Fig. 15b), 1/8° global NLOM (Fig. 15c) and 1/32° global NLOM (Fig. 15d). A significant difference between the NLOM simulations and the 1/12° HYCOM simulation is seen along 48°S east of New Zealand where 1/8° global NLOM simulates an eastward current (Fig. 10a) and both 1/8° and 1/32° NLOM show a corresponding northward rise in SSH vs. a westward current in 1/12° HYCOM (Fig. 13a and b) and a northward decrease in the 1/12° HYCOM and the Maximenko and Niiler mean SSH fields. In another comparison (not shown), the near surface currents simulated by 1/12° HYCOM (Fig. 13a) are in detailed agreement with an analysis of WOCE drifter data presented by Chiswell and Rickard (2006) (their Fig. 6), including westward flow along 48°S feeding into the Southland Current and all of the surface current components related to the Southland Current/SSTF system. This agreement extends to the eastern edge of Fig. 13a (170°W).

Much of the Campbell Plateau and the Chatham Rise are shallower than 600 m and thus intrude into the stratified part of the water column. Given the current along the eastern edge of the Campbell Plateau, the Southland Current/SSTF simulated by 1/12° global HYCOM depends on a gap in the Campbell Plateau that (a) constrains the depth structure of the current system and (b) results in a nonsteric component that provides a strong topographic constraint on the subsequent pathway, including its separation from the western boundary (South Island, NZ). While 1/8° global NLOM simulated a DWBC along the eastern edge of the Campbell Plateau, it failed to simulate the preceding current pathway because it artificially confined crucial topographic features that intruded into the stratified water column to the lowest model layer. In the .72° global HYCOM simulation the northeastward current along the eastern edge of the Campbell Plateau did not extend far enough northward to provide flow through the gap in the Campbell Plateau (not shown) and thus failed to simulate the northeastward Southland Current.

(b–e) Surface layer transport streamfunction (contour interval = .4 Sv) at (b) $t = 0$ years (no abyssal flow, which is turned on at t = 0), (c) $t = 3$ years (initial northward advection of the upper layer streamfunction by the abyssal currents flowing northward along the topographic slope), (d) $t = 7$ years (westward propagation of the northward perturbation in the streamfunction), and (e) $t = 80$ years (a baroclinic western boundary current has formed due solely to the topographically constrained abyssal current).

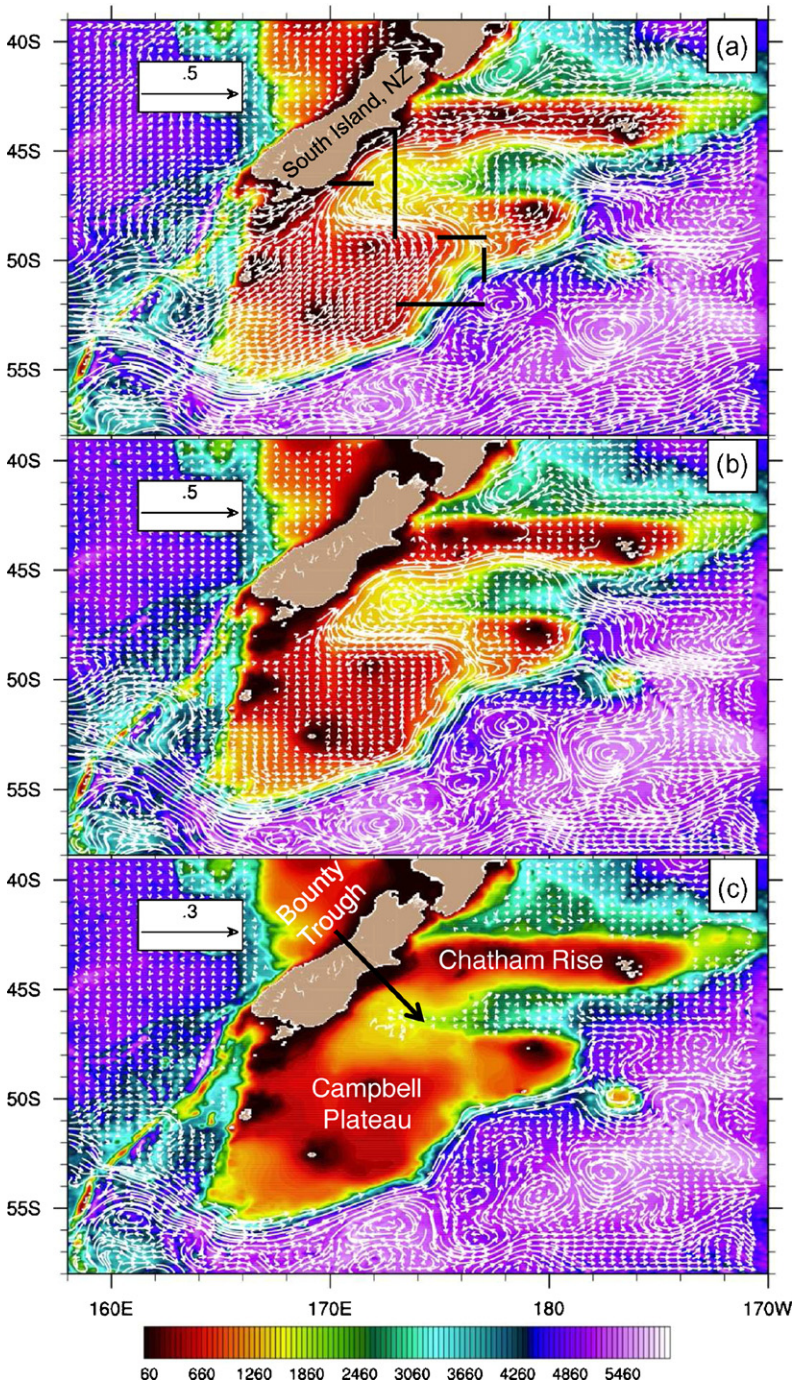

Fig. 13. Mean currents ($m\,s^{-1}$) from 1/12° global HYCOM with 32 layers in the New Zealand region for (a) layer 3 centered at 8.6 m depth, (b) layer 15 centered at ~400 m depth and (c) layer 27 centered at ~3300 m depth. The currents are overlaid on the HYCOM bottom topography. Blank areas occur where the topography is shallower than the HYCOM layer. The 5 black lines plotted on (a) mark the locations of the vertical cross-sections shown in Fig. 14.

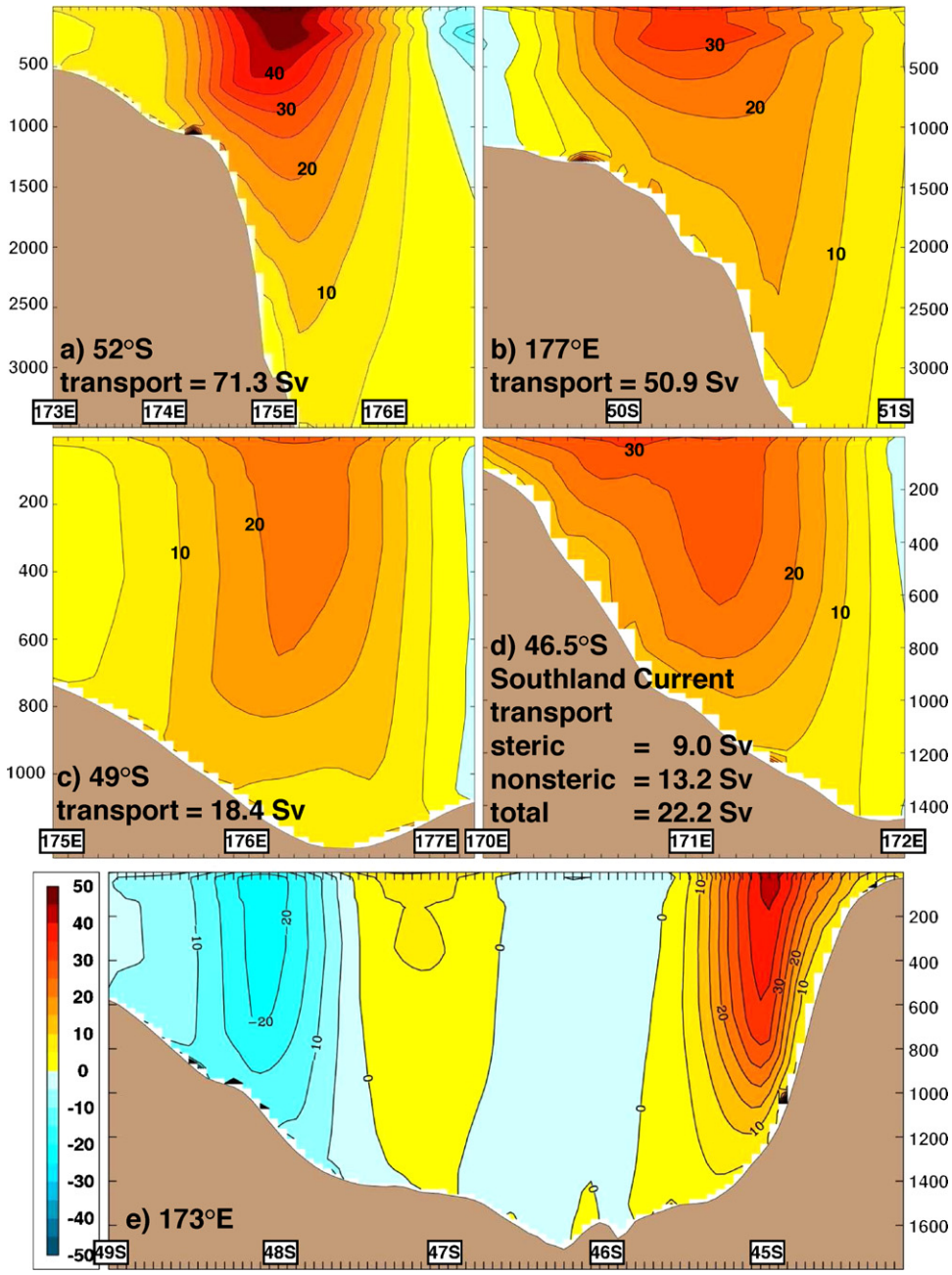

Fig. 14. Cross-sections of mean velocity vs. depth from 1/12° global HYCOM east of South Island, NZ. The locations of the cross-sections are marked in Fig. 13a. The positive mean transports (northward or eastward) through sections (a)–(d) are also given. The observed mean steric transport for the Southland Current (d) is 8.3 Sv with respect to a level of no motion at the bottom (Sutton, 2003) vs. 9.0 Sv in the HYCOM simulation.

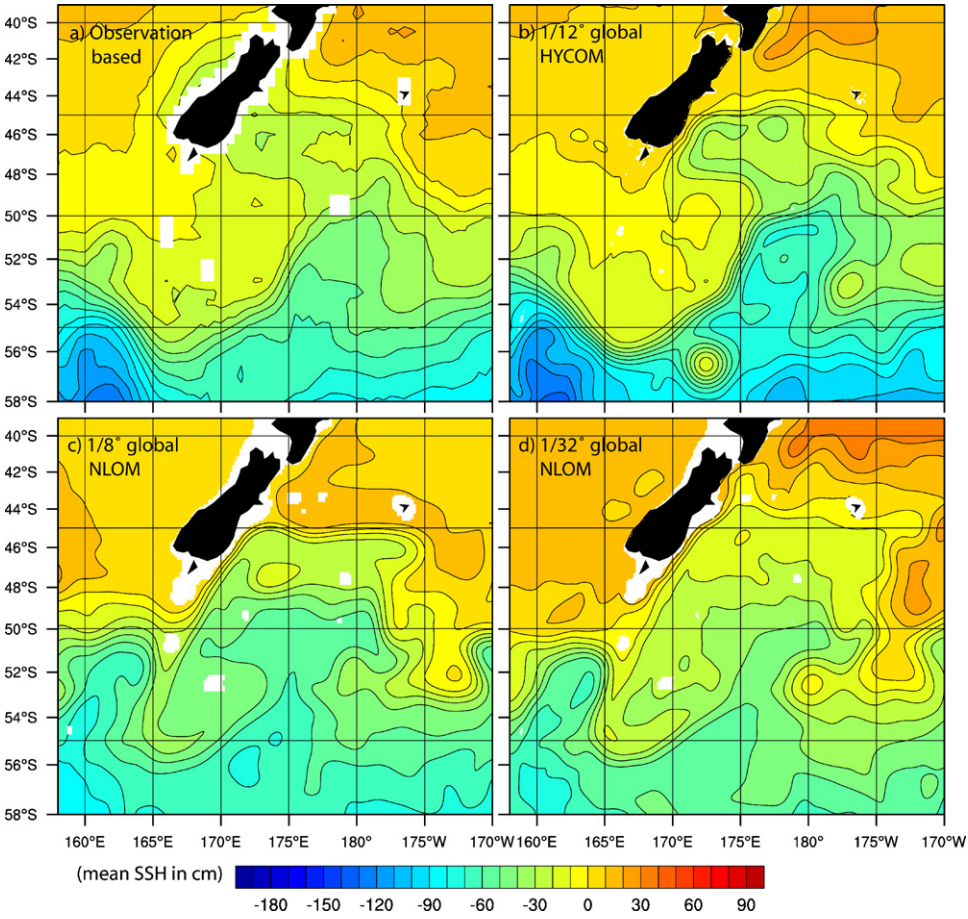

Fig. 15. Mean SSH in the area of southern New Zealand and the Campbell Plateau from (a) the Maximenko and Niiler (2005) global mean based on satellite altimeter, drifting buoy and wind data spanning 1992–2002 and an improved geoid, GRACE (Gravity Recovery and Climate Experiment) Gravity Model (GGM01), (b) a 1/12°, 32-layer global HYCOM simulation forced using an ECMWF ERA40 monthly climatology with wind speed modified using QuikSCAT (see text), (c) a 1/8° global NLOM hydrodynamic simulation used by Tilburg et al. (2001, 2002) forced by the HRsm monthly wind stress climatology, and (d) a 1/32° global NLOM simulation with thermodynamics forced by the HR monthly wind stress climatology. (b–d) are from the same three simulations with bottom topography used throughout Section 4.3.

Does the remote topographic forcing theory of Tilburg et al. (2002) play any role in determining the pathway of the Southland Current/SSTF pathway simulated by 1/12° global HYCOM? HYCOM with 1/12° resolution and 1/8° NLOM simulate Pacific DWBC pathways (Fig. 13c vs. Fig. 10b) that are mostly in basic agreement with the observation-based pathway presented by Carter and Wilkin (1999) over the region they cover, which extends from the southeastern edge of the Campbell Plateau to the eastern edge of the Kermadec Ridge past WOCE line PCM-9 at 32.5°S, where the mean transport below ~3000 m is 11.2 Sv in HYCOM vs. 14.9 Sv observed (Whitworth et al., 1999) or 17.5 Sv observed (Moore and Wilkin, 1998). However, 1/12° HYCOM and 1/8° NLOM simulate significantly different DWBC pathways over the latitude range 44–47°S, where the Southland Current and the eastward current along the SSTF in both models (Figs. 13a and 10a) flow counter to the demands of Sverdrup flow (Fig. 11a and b). In this latitude band, the NLOM DWBC pathway intrudes partway into the Bounty Trough and passes under the SSTF current at the location where the latter separates from the Chatham Rise, a DWBC pathway in close agreement with Carter and Wilkin (1999) and an SSTF pathway consistent with Sutton (2001)

(Fig. 9b). In contrast, the HYCOM DWBC transits 44–47°S northward along ∼170°W (where Carter and Wilkin had minimal data), ∼6° east of the longitude where the HYCOM SSTF current makes its final separation from the Chatham Rise. As a result, the Tilburg et al. (2002) theory for remote topographic forcing of a baroclinic western boundary current cannot be invoked to explain why the Southland Current and the current along the SSTF simulated by HYCOM flow counter to the demands of Sverdrup flow.

Thus, a perfectly good theory by Tilburg et al. (2002) for remote topographic forcing of a baroclinic western boundary current, which applied to their NLOM simulations of the Southland Current and SSTF pathway east of New Zealand, does not apply to the HYCOM results presented here. The Campbell Plateau is one of the few large topographic features in the world ocean where relatively flat topography extends into the stratified ocean, but lies mostly deeper than the nominal 200 m shelf break typical of coastal regions (Fig. 2). As a result, the Campbell Plateau violates a limitation of the two-layer theory employed by Tilburg et al. (2002) (see Section 3), causing it to fail as an explanation of the Southland Current and the SSTF simulated by HYCOM. However, a comparison of the near surface currents in Fig. 13a with the abyssal currents in Fig. 13c reveals a number of places where the abyssal currents steer the pathways of upper ocean currents in areas where the topography lies below the main pycnocline and the conditions of the two-layer theory presented in Section 3 are satisfied.

5. Summary, conclusions, and implications

A wide range of dynamical processes and physical constraints play critical roles in the dynamics of current systems in different regions, including the current systems discussed here. The particular foci of this article are (1) the steering of upper ocean current pathways by topographically constrained abyssal currents that do not impinge on the bottom topography and (2) upper ocean – topographic coupling via flow instabilities. In the latter, baroclinically unstable surface currents (often a mixed barotropic–baroclinic instability) transfer upper ocean energy downward into the abyssal ocean generating eddy-driven deep mean flows that in turn help steer the pathways of upper ocean currents. Although there are other approaches, abyssal current steering of upper ocean currents that do not impinge on the topography can be explained in a particularly clear and direct manner using the continuity equation of a two-layer model. In a two-layer model geostrophic baroclinic currents ($\mathbf{v}_{1g} - \mathbf{v}_{2g}$) are parallel to contours of upper layer thickness (h_1) making $\mathbf{v}_{1g} \cdot \nabla h_1 = \mathbf{v}_{2g} \cdot \nabla h_1$. Thus, in the continuity equation the advection of upper layer thickness gradients by upper and lower layer geostrophic currents is the same. Since typically $|\mathbf{v}_1| \rangle\rangle |\mathbf{v}_2|$, we see that lower layer currents can advect the pathways of upper layer currents, especially where they intersect at large angles. Often the end result of the pathway advection is currents that are nearly parallel because the advection is reduced when this occurs. This process results in a tendency toward barotropy unless there is some mechanism to prevent it, e.g. one that results in a balance between advection and divergence in the layered continuity equation.

This two-layer theory is particularly attractive because it is easy to apply in understanding the dynamics of ocean models ranging from highly idealized to complex eddy-resolving OGCMs designed to simulate a wide range of ocean processes with high vertical resolution. It can also be used in understanding the observed pathways of persistent ocean fronts (over deep water) that are seen in satellite imagery and other data. However, it is essential to consider its range of validity. Clearly, the two-layer theory (1) is designed to explain abyssal current steering of upper ocean current pathways when these currents do not directly impinge on the topography, (2) does not apply when the topography significantly intrudes into the stratified ocean, in which case the flow may be steered directly by the geostrophic contours of the topography, as illustrated in Section 4.3, (3) does not apply when higher vertical modes are important, and (4) does not apply when ageostrophic flow has substantial impact. Thus, this two-layer theory is not likely to work in the tropics where higher vertical modes and ageostrophic flows are more significant. Diapycnal mixing, time dependence, and in means of time-dependent flow, the length of the mean and eddy-mean components of the advection may also affect the results.

In this study we tested the hypothesis that a priori knowledge of the capabilities and limitations of the two-layer theory could be used to predict whether or not it would be consistent with results from an eddy-resolving ocean model with high vertical resolution. The hypothesis was tested (1) by comparing relevant results from eddy-resolving ocean model simulations with high vertical resolution and topography extending through any number of layers to corresponding simulations with low vertical resolution and topography confined to the abyssal layer, and (2) by investigating the success or failure of the theory in explaining the related ocean dynamics in each case. The hypothesis was tested in three regions, two where the a priori knowledge would predict success (the Kuroshio east of Japan and the Japan/East Sea) and a third where a violation of the theory occurs (the Southland Current east of New Zealand). In addition, the significance of the two-layer theory and upper ocean – topographic coupling via flow instabilities in distinguishing between eddy-resolving and eddy-permitting ocean models is discussed in Section 5.1 and in Section 5.2, its role in western boundary current separation from the coast is discussed in relation to other dynamical processes and physical constraints.

Twenty-layer 1/12° HYCOM and six-layer 1/8° NLOM Pacific simulations agreed closely in demonstrating that upper ocean – topographic coupling via flow instabilities plays a key role in simulations of the Kuroshio pathway and its separation from the southeast coast of Japan. Steering by eddy-driven abyssal currents around a modest complex of seamounts just east of the trench is critical to the pathway of Kuroshio separation from the coast and in forming the observed mean northward meander just east of Japan, a feature demonstrated by both models. Near Japan, 1/8° (14 km) resolution was sufficient, but farther to the east 1/16° (7 km) resolution was required even though the first baroclinic Rossby radius of deformation is nearly the same. This resolution increase is needed to obtain greater eastward penetration of the Kuroshio as an inertial jet and the associated upper ocean – topographic coupling via flow instabilities.

In the Japan/East Sea, where the radius of deformation is smaller and the circulation is much weaker, even higher resolution (1/32°, 3.5 km) is required to obtain sufficient upper ocean – topographic coupling via flow instabilities based on a resolution convergence study (up to 1/64° resolution) plus comparisons to an observationally based schematic and observations of mean abyssal currents. In this region there is a strong tendency for the steering by abyssal currents to adjust the upper ocean circulation toward barotropy during the upper ocean – topographic coupling process with the end result that mean upper ocean currents tend to parallel the mean abyssal circulation and topographic slopes in many places, e.g. along much of the subpolar front. Despite the strong upper ocean – topographic coupling over much of the basin, a comparison of simulations forced by six different wind stress climatologies showed the choice of wind forcing product can have a substantial impact on the simulated circulation, e.g. the dynamical mechanism for separation from the western boundary, the relative strength of the subpolar front and the Tsushima Warm Current off the northern coast of Japan, and the pathways of current segments. The differences between these simulations are also affected by upper ocean – topographic coupling. The preceding results from a 4-layer model were applicable to a 15-layer HYCOM simulation where the visual and statistical match between the surface circulation of the 15-layer HYCOM and 4-layer NLOM simulations with the same wind forcing was generally much closer than the match between the same NLOM simulation and the NLOM simulations forced by the five other wind products. This information is useful in understanding the preferred locations for intrathermocline eddy formation in the 15-layer HYCOM simulation, a phenomenon the 4-layer model could not simulate.

The Campbell Plateau has a major impact on the ocean circulation east and southeast of South Island, New Zealand and a critical impact on the dynamics of the Southland Current. It also provides an example where the two-layer theory is not applicable. The Southland Current flows along a segment of the south subtropical front (SSTF) on the eastern side of South Island, NZ. In particular, it flows northeastward, counter to the demands of Sverdrup flow as shown in global linear simulations and counter to the direction depicted in global nonlinear 1/8° flat bottom and reduced gravity NLOM simulations and a non-eddy-resolving .72° global HYCOM simulation. The linear solution consists of Sverdrup flow with Munk western boundary layers and is in accord with Godfrey's rule for the treatment of islands. Using output from NLOM, Tilburg et al. (2002) explained the Southland Current by a different mechanism for the formation of a baroclinic western boundary current, remote topographic forcing. The South Pacific Deep Western Boundary Current flows equatorward along the southeastern

edge of the Campbell Plateau. It passes under the SSTF ∼12° east of New Zealand, locally advecting it northward to the southern edge of the Chatham Rise. The western edge of this northward perturbation then propagates westward as a non-dispersive internal Rossby wave until it reaches the eastern coastal region of South Island, NZ. There, it equilibrates as the Southland Current and an SSTF along the southern edge of the Chatham Rise, in accord with observations. However, a three-way comparison of larger scale observed SSH and output from HYCOM and NLOM revealed that NLOM fails to simulate a second observed pathway feeding into the Southland Current.

The Campbell Plateau and the Chatham Rise are rare features of the global ocean where the topography is shallow enough that it intrudes into the stratified part of the water column over a substantial area, but lies deeper than the typical 200 m continental shelf break depth, thus violating an assumption of the two-layer theory. In HYCOM the depth of the topography is accurately represented, while in NLOM vertically compressed but otherwise realistic topography is confined to the lowest layer, which lies beneath the stratified ocean. As a result, the dynamics of the HYCOM and NLOM simulations are very different in this region. Although a perfectly good theory was used to explain the NLOM results, unrealistic behavior of the NLOM simulation led to an inappropriate dynamical interpretation of the true circulation pattern. Overall, the HYCOM results agreed much better with observations and HYCOM did simulate the second observed pathway, which is dominant in HYCOM. This pathway originates from the subantarctic front as a current along the eastern edge of the Campbell Plateau. A portion of the current flowing above isobaths shallower than the 1200 m sill depth passes through a gap in the Campbell Plateau and the sill of the gap constrains the depth structure of the downstream current. This constraint adds a strong barotropic component that steers the cyclonic, U-shaped downstream pathway along geostrophic contours around the Bounty Trough, first westward to the coast of South Island, NZ, second merging with a shallow current from the southwest to become the northeastward Southland Current along the coast, and third separating from the coast to follow the SSTF along the southern slope of the Chatham Rise.

In conclusion, the results of the hypothesis testing in three regions are consistent with the a priori knowledge of the capabilities and limitations of the two-layer theory for abyssal current steering of upper ocean current pathways and upper ocean – topographic coupling via flow instabilities. In the two regions of anticipated validity the relevant results from the eddy-resolving ocean model simulations with high and low vertical resolution demonstrated good agreement and yielded a consistent interpretation of the related ocean dynamics. In the region where the theory was violated the results from the two models were clearly inconsistent and the high vertical resolution simulation was inconsistent with the theory. The low vertical resolution simulation was consistent with the theory because the topography was confined to the lowest layer, when in reality the topography intruded well into the stratified water column, violating a limitation of the two-layer theory. In this region an alternate dynamical explanation of the high vertical resolution simulation was presented.

5.1. Implications for eddy-resolving vs. eddy-permitting ocean models

In general, the model simulations show increasingly widespread importance of mesoscale flow instabilities in allowing bottom topography to steer the pathways of upper ocean currents, as the horizontal resolution of the model is increased. This upper ocean – topographic coupling requires that mesoscale variability and related flow instabilities be very well resolved to obtain sufficient coupling, e.g. to achieve accurate representation of the vortex stretching and compression associated with baroclinic instability in the presence of realistic topography. Thus, this eddy-driven topographic effect is missed at coarser resolution and can lead to unexplained errors in simulations of mean upper ocean current pathways and to false conclusions about the influence of topography. Resolving the first baroclinc Rossby radius of deformation has been used as a criterion for distinguishing between eddy-permitting and eddy-resolving models because of its relation to the predominant space scale for baroclinic instability. However, the results presented here suggest that refinement is needed in making the distinction between eddy-permitting and eddy-resolving, one that goes beyond the internal Rossby radius of deformation and also considers (1) the need for increased resolution to simulate sufficient eastward penetration of inertial jets (where needed), (2) resolution convergence for the mean strength and pathways of upper ocean and abyssal currents (and their variability statistics), and (3)

comparisons to observations of mean upper ocean and abyssal currents and their variability statistics, including the basic characteristics of eddies and their behavior (when relevant).

At a minimum the radius of deformation and the need for realistic simulation of the eastward penetration of inertial jets and associated nonlinear recirculation gyres influence the horizontal resolution required, the latter both from (a) the effect on the inertial character of jets and recirculation gyres and from (b) their influence on flow instabilities and the eddy-driven abyssal circulation. In a given region ocean model transition from eddy-permitting with a minimal eddy-driven mean abyssal circulation to eddy-resolving with a robust eddy-driven abyssal circulation that supports upper ocean – topographic coupling via flow instabilities typically occurs over one doubling of the resolution. An additional doubling of the resolution can have significant effects, especially effects related to the simulation of inertial jets and their nonlinear recirculation gyres. These results make upper ocean – topographic coupling via flow instabilities a key dynamical phenomenon in distinguishing between eddy-resolving and eddy-permitting ocean models and make it essential in meeting the criteria given above in regions where it may occur. The extent to which it occurs is yet to be determined, but major upper ocean current systems are not required, as evidenced in the Japan/East Sea. Further, the resolution required for it to occur can vary under the influence of multiple factors, from 3.5 to 14 km in the results discussed here.

In contrast, baroclinic instability requires a minimum of two vertical modes, the barotropic and first baroclinic in these applications. In addition, the two-layer theory for abyssal current steering of upper ocean current pathways and the upper ocean – topographic coupling via flow instabilities require dominance of the barotropic and first baroclinic modes. Accordingly, the results for upper ocean – topographic coupling exhibit low sensitivity to the vertical resolution as demonstrated by the NLOM–HYCOM comparisons for the Kuroshio (6 vs. 20 layers) and the Japan/East Sea (4 vs. 15 layers) discussed here and by the extensive and detailed model-data comparisons for the Gulf Stream and regional abyssal circulation simulated by a five-layer model (Hurlburt and Hogan, 2000, 2008, this issue). Consistent with low sensitivity to vertical resolution associated with the preceding processes, HYCOM makes the transition from eddy-permitting to eddy-resolving at essentially the same horizontal resolution as NLOM. Based on the regions studied so far and observation-based estimates of the first baroclinic Rossby radius of deformation covering most of the global ocean from Emery et al. (1984), Chelton et al. (1998), and Oh et al. (2000), a realistic global OGCM with 1/25° equatorial (3.5 km mid-latitude) resolution should be capable of simulating upper ocean – topographic coupling via flow instabilities, its impacts on the pathways of upper ocean currents and fronts, and its influences on boundary current separation from the coast nearly anywhere they occur. That includes the capability to provide realistic simulations of all the regions discussed here and the Gulf Stream region discussed by Hurlburt and Hogan (2008, this issue), given realistic atmospheric forcing, seafloor topography, and parameterized mixing processes.

5.2. Implications for western boundary current separation from the coast

The dynamics of boundary current separation from the coast are important in all four of the regions discussed here (Gulf of Mexico, Kuroshio, Japan/East Sea, and east of South Island, NZ) and in the Gulf Stream region discussed in a companion article (Hurlburt and Hogan, 2008, this issue). Four of these currents separate from a western boundary and then flow generally eastward. In the Gulf of Mexico the Loop Current flows northward as an inertial jet as it separates. Although highly time-dependent, its separation pathway is nominally governed by the space scale for westward bending of the northward jet $(v_c/\beta)^{1/2}$, where v_c is the speed at the core of the current and B is the variation of the Coriolis parameter with latitude (Hurlburt and Thompson, 1980). The Kuroshio, the East Korea Warm Current, and the Gulf Stream all separate from the western boundary as inertial jets with separation pathways influenced by wind stress curl and upper ocean – topographic coupling via flow instabilities associated with specific topographic features. Although these currents are influenced by some of the same dynamical processes, the roles these processes play in the overall separation dynamics differ significantly in each region and in each case additional dynamical processes and physical constraints, not shared in common, affect the overall separation dynamics.

As brief examples, boundary current separation in the Japan/East Sea is also influenced by flow through the straits connecting it with the Pacific Ocean and by the existence of the Tsushima Warm Current along the north coast of Japan. In addition, the choice of wind forcing product or interannual variability in the forcing determines whether or not realistic separation from the western boundary depends on anticyclonic abyssal flow around a specific rise in the seafloor just east of Korea, although the downstream pathway depends on abyssal current steering in all of the eddy-resolving (3.5 km resolution) simulations. The strength of the Gulf Stream as an inertial jet is enhanced by the meridional overturning circulation. Its separation from the western boundary at Cape Hatteras also depends on the orientation of the coastline near separation, an approximate constant absolute vorticity (CAV) trajectory between the separation point at 35.5°N, 75°W and ∼70°W, abyssal current steering of the pathway by a specific topographic feature near 68–69°W, conservation of potential vorticity as the abyssal current passes under the Gulf Stream, and a resulting feedback that locally prevents further southward abyssal current advection of the Gulf Stream. Thus, the Gulf Stream helps determine its own latitude at ∼68.5°W, a constraint needed for realistic separation from the western boundary via an approximate CAV trajectory (based on results from Hurlburt and Hogan, 2008, this issue). The Southland Current along the east coast of South Island, NZ flows northeastward, counter to the demands of Sverdrup flow. Given a boundary current along the eastern edge of the Campbell Plateau, separation of the Southland Current from the coast of South Island depends on a trough in the seafloor between the Campbell Plateau and the Chatham Rise just east of the island and flow through a gap in the Campbell Plateau. The ∼1200 m sill depth of the gap determines the vertical structure of the current and adds a strong nonsteric component that constrains the current to follow the geostrophic contours of the trough, a pathway that includes separation from the coastal boundary. Thus, while some commonalities exist, the separation dynamics of the different boundary currents demonstrate substantial differences. See the related sections and Hurlburt and Hogan (2008, this issue) for references and additional discussion of these results.

Acknowledgements

This article is a contribution to the 6.1 project Global Remote Littoral Forcing via Deep Water Pathways and to the 6.1 Japan/East Sea Directed Research Initiative (DRI), both sponsored by the Office of Naval Research (ONR) under program element 601153N. Grants of both “challenge” and “non-challenge” computer time were provided by the Department of Defense High Performance Computing Modernization Program. We thank guest editor, Igor Belkin, for his invitation to write an article for this special issue. Originally a review article was requested. Instead, in the present article previously published results from ocean models with low vertical resolution are compared with new results from high vertical resolution simulations to investigate the applicability of a two-layer theory in understanding the dynamics of high vertical resolution models. We thank the reviewers whose comments led to major improvements in this article. We thank Alan Wallcraft for his computer expertise and his developmental work on both the HYbrid Coordinate Ocean Model (HYCOM) and the NRL Layered Ocean Model (NLOM). We also thank Birol Kara for his work in developing and evaluating the Quickscat-modified ERA40 winds used in forcing some of the simulations. In addition, we thank Charlene Parker for her assistance. This is contribution NRL/JA/7304-06-6342 and has been approved for public release.

References

Belkin, I.M., 1988. Main hydrological features of the central South Pacific. In: Vinogradov, M.E., Flint, M.V. (Eds.), Ekosistemy Subantarkticheskoy Zony Tikhogo Okeana (Ecosystems of the Subantarctic Zone of the Pacific Ocean). Nauka, Moscow, pp. 21–28 (in Russian).

Belkin, I.M., Gordon, A.L., 1996. Southern Ocean fronts from the Greenwich meridian to Tasmania. J. Geophys. Res. 101 (C2), 3675–3696.

Bleck, R., 2002. An ocean general circulation model framed in hybrid isopycnic–Cartesian coordinates. Ocean Model. 4, 55–88.

Bleck, R., Benjamin, S.G., 1993. Regional weather prediction with a model combining terrain-following and isentropic coordinates. 1. Model description. Mon. Weather Rev. 121 (6), 1770–1785.

Bleck, R., Boudra, D.B., 1981. Initial testing of a numerical ocean circulation model using a hybrid (quasi–isopycnic) vertical coordinate. J. Phys. Oceanogr. 11 (6), 755–770.

Bleck, R., Smith, L.T., 1990. A wind-driven isopycnic coordinate model of the North and Equatorial Atlantic Ocean. 1. Model development and supporting experiments. J. Geophys. Res. 95 (C3), 3273–3285.
Carter, L., Wilkin, J., 1999. Abyssal circulation around New Zealand—a comparison between observations and a global circulation model. Mar. Geol. 159 (1–4), 221–239.
Chang, K.I., Hogg, N.G., Suk, M.S., Byun, S.K., Kim, Y.G., Kim, K., 2002. Mean flow and variability in the southwestern East Sea. Deep Sea Res. I 49 (12), 2261–2279.
Chang, K.I., Teague, W.J., Lyu, S.J., Perkins, H.T., Lee, D.K., Watts, D.R., Kim, Y.B., Mitchell, D.A., Lee, C.M., Kim, K., 2004. Circulation and currents in the southwestern East/Japan Sea: overview and review. Prog. Oceanogr. 61 (2–4), 105–156.
Chassignet, E.P., Hurlburt, H.E., Smedstad, O.M., Halliwell, G.R., Hogan, P.J., Wallcraft, A.J., Bleck, R., 2007. Ocean prediction with the HYbrid Coordinate Ocean Model (HYCOM). J. Mar. Sys. 65 (1–4), 60–83.
Chassignet, E.P., Hurlburt, H.E., Smedstad, O.M., Halliwell, G.R., Wallcraft, A.J., Metzger, E.J., Blanton, B.O., Lozano, C., Rao, D.B., Hogan, P.J., Srinivasan, A., 2006. Generalized vertical coordinates for eddy-resolving global and coastal ocean forecasts. Oceanography 19 (1), 118–129.
Chassignet, E.P., Smith, L.T., Halliwell, G.R., Bleck, R., 2003. North Atlantic simulation with the HYbrid Coordinate Ocean Model (HYCOM): impact of the vertical coordinate choice, reference density, and thermobaricity. J. Phys. Oceanogr. 33, 2504–2526.
Chiswell, S.M., Rickard, G.J., 2006. Comparison of model and observational ocean circulation climatologies for the New Zealand region. J. Geophys. Res. 111, C10011, doi:10.1029/2006JC003489.
Chelton, D.B., deSzoeke, R.A., Schlax, M.G., 1998. Geographical variability of the first baroclinic Rossby radius of deformation. J. Phys. Oceanogr. 28 (3), 433–460.
Emery, W.J., Lee, W.G., Magaard, L., 1984. Geographic and seasonal distributions of Brunt-Vaisala frequency and Rossby radii in the North Pacific and North Atlantic. J. Phys. Oceanogr. 14, 294–317.
Gibson, J.K., Kallberg, P., Uppala, S., Hernandez, A., Nomura, A., Serrano, E., 1997. ECMWF Re-Analysis Project Report Series: 1. ERA Description. ECMWF, Reading, Berkshire, UK.
Godfrey, J.S., 1989. A Sverdrup model of the depth-integrated flow for the world ocean allowing for island circulations. Geophys. Astrophys. Fluid Dyn. 45 (1–2), 89–112.
Gordon, A.L., Giulivi, C.F., Lee, C.M., Furey, H.H., Bower, A., Talley, L., 2002. Japan/East Sea intrathermocline eddies. J. Phys. Oceanogr. 32 (6), 1960–1974.
Hallock, Z.R., Teague, W.J., 1996. Evidence for a North Pacific deep western boundary current. J. Geophys. Res. 101 (C3), 6617–6624.
Hellerman, S., Rosenstein, M., 1983. Normal monthly wind stress over the world ocean with error estimates. J. Phys. Oceanogr. 13, 1093–1104.
Hogan, P.J., Hurlburt, H.E., 2000. Impact of upper ocean – topographic coupling and isopycnal outcropping in Japan/East Sea models with 1/8° to 1/64° resolution. J. Phys. Oceanogr. 30, 2535–2561.
Hogan, P.J., Hurlburt, H.E., 2005. Sensitivity of simulated circulation to surface wind forcing in the Japan/East Sea. Deep Sea Res. 52, 1464–1489.
Hogan, P.J., Hurlburt, H.E., 2006. Why do intrathermocline eddies form in the Japan/East Sea? A modeling perspective. Oceanography 19 (3), 134–143.
Holland, W.R., 1973. Baroclinic and topographic influences on the transport in western boundary currents. Geophys. Fluid Dyn. 4, 187–210.
Holland, W.R., 1978. The role of mesoscale eddies in the general circulation of the ocean—numerical experiments using a wind-driven quasi-geostrophic model. J. Phys. Oceanogr. 8, 363–392.
Holland, W.R., Lin, L.B., 1975. Generation of mesoscale eddies and their contribution to oceanic general circulation. 1. Preliminary numerical experiment. J. Phys. Oceanogr. 5 (4), 642–657.
Hurlburt, H.E., Chassignet, E.P., Cummings, J.A., Kara, A.B., Metzger, E.J., Shriver, J.F., Smedstad, O.M., Wallcraft, A.J., Barron, C.N., 2008. Eddy-resolving global ocean prediction. In: Hecht, M., Hasumi, H. (Eds.), Ocean Modeling in an Eddying Regime, Geophysical Monograph 177. American Geophysical Union, Washington, DC.
Hurlburt, H.E., Hogan, P.J., 2000. Impact of 1/8° to 1/64° resolution on Gulf Stream model-data comparisons in basin-scale subtropical Atlantic Ocean models. Dyn. Atmos. Oceans 32, 283–329.
Hurlburt, H.E., Hogan, P.J., 2008. The Gulf Stream pathway and the impacts of the eddy-driven abyssal circulation and the Deep Western Boundary Current. Dyn. Atmos. Oceans 45, 71–101.
Hurlburt, H.E., Metzger, E.J., 1998. Bifurcation of the Kuroshio Extension at the Shatsky Rise. J. Geophys. Res. 103 (C4), 7549–7566.
Hurlburt, H.E., Metzger, E.J., Hogan, P.J., 1997. The impact of upper ocean – topographic coupling on the Kuroshio pathway south and east of Japan. International WOCE Newsletter, Number 25, pp. 19–20, 23,25.
Hurlburt, H.E., Thompson, J.D., 1980. A numerical study of Loop Current intrusions and eddy shedding. J. Phys. Oceanogr. 10, 1611–1651.
Hurlburt, H.E., Thompson, J.D., 1982. The dynamics of the Loop Current and shed eddies in a numerical model of the Gulf of Mexico. In: Nihoul, J.C.J. (Ed.), Hydrodynamics of Semi-Enclosed Seas. Elsevier, New York, pp. 243–297.
Hurlburt, H.E., Thompson, J.D., 1984. Preliminary results from a numerical study of the New England Seamount Chain influence on the Gulf Stream. In: Holloway, G., West, B.J. (Eds.), Predictability of Fluid Motions, Am. Inst. Physics Conf. Proc. 106. American Institute of Physics, New York, pp. 489–503.
Hurlburt, H.E., Wallcraft, A.J., Schmitz Jr., W.J., Hogan, P.J., Metzger, E.J., 1996. Dynamics of the Kuroshio/Oyashio current system using eddy-resolving models of the North Pacific Ocean. J. Geophys. Res. 101 (C1), 941–976.
Kallberg, P., Simmons, A., Uppala, S., Fuentes, M., 2004. ERA-40 Project Report Series: 17. The ERA-40 archive. ECMWF, Reading, Berkshire, UK.
Kalnay, E., Kanamitsu, M., Kistler, R., Collins, W., Deaven, D., Gandin, L., Iredell, M., Saha, S., White, G., Woollen, J., Zhu, Y., Chelliah, M., Ebisuzaki, W., Higgins, W., Janowiak, J., Mo, K.C., Ropelewski, C., Wang, J., Leetmaa, A., Reynolds, R., Jenne, R., Joseph, D., 1996. The NCEP/NCAR 40-year reanalysis project. Bull. Am. Met. Soc. 77 (3), 437–471.
Kara, A.B., Hurlburt, H.E., 2006. Daily inter-annual simulations of SST and MLD using atmospherically forced OGCMs: model evaluation in comparison to buoy time series. J. Mar. Sys. 62, 95–119.

Kara, A.B., Hurlburt, H.E., Wallcraft, A.J., 2005. Stability-dependent exchange coefficients for air-sea fluxes. J. Atmos. Oceanic Technol. 22, 1080–1094.
Kara, A.B., Rochford, P.A., Hurlburt, H.E., 2002. Air-sea flux estimates and the 1997–1998 ENSO event. Boundary-Layer Meteorol. 103, 439–458.
Kara, A.B., Wallcraft, A.J., Hurlburt, H.E., 2003. Climatological SST and MLD predictions from a global layered ocean model with an embedded mixed layer. J. Atmos. Oceanic Technol. 20, 1616–1632.
Ko, D.-S., 2002. NRL DBDB2 global 2-minute topography. http://www7320.nrlssc.navy.mil/DBDB2_WWW.
Maximenko, N.A., Niiler, P.P., 2005. Hybrid decade-mean global sea level with mesoscale resolution. In: Saxena, N. (Ed.), Recent Advances in Marine Science and Technology, 2004. PACON International, Honolulu, pp. 55–59.
Metzger, E.J., Hurlburt, H.E., 1996. Coupled dynamics of the South China Sea, the Sulu Sea, and the Pacific Ocean. J. Geophys. Res. 101 (C5), 12331–12352.
Morimoto, A., Yanagi, T., 2001. Variability of sea surface circulation in the Japan Sea. J. Oceanogr. 57, 1–13.
Moore, D.R., Wallcraft, A.J., 1998. Formulation of the NRL Layered Ocean Model in spherical coordinates, NRL CR 7323-96-0005. Nav. Res. Lab., Stennis Space Center, MS.
Moore, M.I., Wilkin, J.L., 1998. Variability in the South Pacific Deep Western Boundary Current from current meter observations and a high-resolution global model. J. Geophys. Res. 103 (C3), 5439–5457.
Munk, W.H., 1950. On the wind-driven ocean circulation. J. Met. 7 (2), 79–93.
Na, J.-Y., Seo, J.-W., Han, S.K., 1992. Monthly mean sea surface winds over the adjacent seas of the Korea peninsula. J. Oceanolog. Soc. Korea 27, 1–10.
Na, J.-Y., Seo, J.-W., Lie, H.-J., 1999. Annual and seasonal variations of the sea surface heat fluxes in the East Asian marginal seas. J. Oceanogr. 55, 257–270.
Niiler, P.P., Maximenko, N.A., McWilliams, J.C., 2003. Dynamically balanced absolute sea level of the global ocean derived from near-surface velocity observations. Geophys. Res. Lett. 30 (22), 2164, doi:10.1029/2003GL018628.
Oh, I.S., Zhurbas, V., Park, W.S., 2000. Estimating horizontal diffusivity in the East Sea (Sea of Japan) and the northwest Pacific from satellite-tracked drifter data. J. Geophys. Res. 105 (C3), 6483–6492.
Preller, R.H., Hogan, P.J., 1998. Oceanography of the Sea of Okhotsk and the Japan/East Sea. In: Robinson, A.R., Brink, K.H. (Eds.), The Sea: The Global Coastal Ocean, Regional Studies and Synthesis, 11. Wiley, New York, pp. 429–481.
Rosmond, T.E., Teixeira, J., Peng, M., Hogan, T.F., Pauley, R., 2002. Navy Operational Global Atmospheric Prediction System (NOGAPS): forcing for ocean models. Oceanography 15 (1), 99–108.
Senyu, T., 1999. The Japan Sea intermediate water; its characteristics and circulation. J. Oceanogr. 55, 111–122.
Shriver, J.F., Hurlburt, H.E., Smedstad, O.M., Wallcraft, A.J., Rhodes, R.C., 2007. 1/32° real-time global ocean prediction and value-added over 1/16° resolution. J. Mar. Sys. 65 (1–4), 3–26.
Smedstad, O.M., Hurlburt, H.E., Metzger, E.J., Rhodes, R.C., Shriver, J.F., Wallcraft, A.J., Kara, A.B., 2003. An operational eddy-resolving 1/16° global ocean nowcast/forecast system. J. Mar. Sys. 40–41, 341–361.
Spall, M.A., 1996. Dynamics of the Gulf Stream/Deep Western Boundary Current crossover. Part I: Entrainment and recirculation. J. Phys. Oceanogr. 26, 2152–2168.
Sutton, P., 2001. Detailed structure of the Subtropical Front over Chatham Rise, east of New Zealand. J. Geophys. Res. 106 (C12), 31045–31056.
Sutton, P.J.H., 2003. The Southland Current: a subantarctic current. N.Z.J. Mar. Freshwater Res. 37, 645–652.
Sverdrup, H.U., 1947. Wind-driven currents in a baroclinic ocean—with application to the equatorial currents of the eastern Pacific. Proc. Natl. Acad. Sci. U.S.A. 33 (11), 318–326.
Tansley, C.E., Marshall, D.P., 2000. On the influence of bottom topography and the Deep Western Boundary Current on Gulf Stream separation. J. Mar. Res. 58, 297–325.
Teague, W.J., Carron, M.J., Hogan, P.J., 1990. A comparison between the generalized digital environmental model and Levitus climatologies. J. Geophys. Res. 95 (C5), 7167–7183.
Teague, W.J., Tracey, K.L., Watts, D.R., Book, J.W., Chang, K.I., Hogan, P.J., Mitchell, D.A., Suk, M.S., Wimbush, M., Yoon, J.H., 2005. Observed deep circulation in the Ulleung Basin. Deep Sea Res. II 52 (11–13), 1802–1826.
Thompson, J.D., Schmitz Jr., W.J., 1989. A regional primitive-equation model of the Gulf Stream: design and initial experiments. J. Phys. Oceanogr. 19, 791–814.
Tilburg, C.E., Hurlburt, H.E., O'Brien, J.J., Shriver, J.F., 2001. The dynamics of the East Australian Current system: the Tasman Front, the East Auckland Current and the East Cape Current. J. Phys. Oceanogr. 31, 2917–2943.
Tilburg, C.E., Hurlburt, H.E., O'Brien, J.J., Shriver, J.F., 2002. Remote topographic forcing of a baroclinic western boundary current: an explanation for the Southland Current and the pathway of the subtropical front east of New Zealand. J. Phys. Oceanogr. 32 (11), 3216–3232.
Uddstrom, M.J., Oien, N.A., 1999. On the use of high-resolution satellite data to describe the spatial and temporal variability of sea surface temperatures in the New Zealand region. J. Geophys. Res. 104 (C9), 20729–20751.
Wallcraft, A.J., 1991. The Navy Layered Ocean Model users guide, NOARL Report 35. Nav. Res. Lab., Stennis Space Center, MS.
Wallcraft, A.J., Kara, A.B., Hurlburt, H.E., Rochford, P.A., 2003. The NRL Layered Ocean Model (NLOM) with an embedded mixed layer sub-model: formulation and tuning. J. Atmos. Oceanic Technol. 20, 1601–1615.
Wallcraft, A.J., Moore, D.R., 1997. The NRL Layered Ocean Model. Parallel Comput. 23, 2227–2242.
Whitworth III, T., Warren, B.A., Nowlin Jr., W.D., Rutz, S.B., Pillsbury, R.D., Moore, M.I., 1999. On the deep western-boundary current in the Southwest Pacific Basin. Prog. Oceanogr. 43, 1–54.